

1 Small-molecule inhibitors of the PDZ domain of Dishevelled 2 proteins interrupt Wnt signalling

3
4 Nestor Kamdem ^{1,2}, Yvette Roske ³, Dmytro Kovalsky ^{4,6}, Maxim O. Platonov ^{4,6}, Oleksii
5 Balinskyi ^{4,6}, Annika Kreuchwig ^{1,2}, Jörn Saupe ^{1,2}, Liang Fang ^{2,3}, Anne Diehl ¹, Peter
6 Schmieder ¹, Gerd Krause ¹, Jörg Rademann ^{1,5}, Udo Heinemann ^{2,3}, Walter Birchmeier ³ and
7 Hartmut Oschkinat ^{1,2}.

8
9 ¹ Leibniz-Forschungsinstitut für Molekulare Pharmakologie, Robert-Rössle-Straße 10, 13125 Berlin, Germany

10 ² Institut für Chemie und Biochemie, Freie Universität Berlin, Takustraße 3, 14195 Berlin, Germany

11 ³ Max-Delbrück-Center for Molecular Medicine, Robert-Rössle-Straße 10, 13125 Berlin, Germany

12 ⁴ Enamine Ltd., Chervonotkatska Street 78, Kyiv 02094, Ukraine

13 ⁵ Institut für Pharmazie, Freie Universität Berlin, Königin-Luise-Straße 2 + 4, 14195 Berlin, Germany

14 ⁶ Taras Shevchenko National University, 62 Volodymyrska, Kyiv 01033, Ukraine

15
16 Correspondence to: Hartmut Oschkinat (oschkinat@fmp-berlin.de)

Feldfunktion geändert

18 Abstract

19 Dishevelled (Dvl) proteins are important regulators of the Wnt signalling pathway, interacting through
20 their PDZ domains with the Wnt receptor Frizzled. Blocking the Dvl PDZ/Frizzled interaction represents
21 a potential approach for cancer treatment, which stimulated the identification of small molecule
22 inhibitors, among them the anti-inflammatory drug Sulindac and Ky-02327. Aiming to develop tighter
23 binding compounds without side effects, we investigated structure-activity relationships of
24 sulfonamides. X-ray crystallography showed high complementarity of anthranilic acid derivatives in the
25 GLGF loop cavity and space for ligand growth towards the PDZ surface. Our best binding compound
26 inhibits Wnt signalling in a dose-dependent manner as demonstrated by TOP-GFP assays ($IC_{50} \sim 50 \mu M$),
27 and Western blotting of β -catenin levels. Real-time PCR showed reduction in the expression of Wnt-
28 specific genes. Our compound interacted with Dvl-1 PDZ ($K_D = 2.4 \mu M$) stronger than Ky-02327 and
29 may be developed into a lead compound interfering with the Wnt pathway.

hat gelöscht: a

30

31

32 KEYWORDS: Drug Design, NMR, PDZ, Frizzled, Wnt signalling

33

35 INTRODUCTION

36 [Dishevelled \(Dvl\) proteins comprise 500 to 600 amino acids and contain three conserved domains: an](#)
37 [N-terminal DIX \(Dishevelled/Axin\) domain \(Schwarz-Romond 2007, Madrzak 2015\), a central PDZ](#)
38 [\(PSD95/Dlg1/ZO-1\) domain \(Doyle 1996, Ponting 1997\), and a C-terminal DEP \(Dishevelled/Egl-](#)
39 [10/Pleckstrin\) domain \(Wong 2000, Wallingford 2005\). Dvl transduces Wnt signals from the membrane](#)
40 [receptor Frizzled to downstream components *via* the interaction between Dvl PDZ and Frizzled \(Wong](#)
41 [2003\), thus it has been proposed as drug target \(Klaus 2008, Holland 2013, Polakis 2012\). Several](#)
42 [studies identified internal peptides of the type \(KTXXXW\) as well as C-terminal peptides of the type](#)
43 [\(\$\Omega\$ \$\Phi\$ GW \$\Phi\$ \) in which \$\Omega\$ is any aromatic amino acid \(F, W or Y\) as Dvl PDZ targets \(Lee 2009, Zhang](#)
44 [2009\). Three Dvl homologues, Dvl-1, Dvl-2 and Dvl-3, have been identified in humans. Sequence](#)
45 [identity is 88% between Dvl-3 PDZ and Dvl-1 PDZ and 96% between Dvl-3 PDZ and Dvl-2 PDZ](#)
46 [\(Supporting Information Figure S1\). Dvl proteins are found to be upregulated in breast, colon, prostate,](#)
47 [mesothelium, and lung cancers \(Weeraratna 2002, Uematsu 2003, Bui 1997, Mizutani 2005\).](#)

48 [PDZ domains appear in 440 copies spread over more than 260 proteins of the human proteome \(Ponting](#)
49 [1997\). They maintain relatively specific protein-protein interactions and are involved, for example, in](#)
50 [signalling pathways, membrane trafficking and in the formation of cell-cell junctions \(Zhang 2003,](#)
51 [Fanning 1996, Kurakin 2007\). Hence, they are potentially attractive drug targets \(Rimbault 2019,](#)
52 [Christensen 2020\). PDZ domains consist of about 90 amino acids which fold into two \$\alpha\$ -helices and six](#)
53 [\$\beta\$ -strands exposing a distinct peptide-binding groove \(Doyle 1996\), Lee 2017\). The conserved](#)
54 [carboxylate-binding loop \(GLGF loop, **FLGI in Dvl-2 and -3, Figure 1**\) is essential for the formation of](#)
55 [a hydrogen bonding network between the PDZ domain and PDZ-binding, C-terminal peptide motifs, in](#)
56 [most cases coordinating the C-terminal carboxylate group of the interaction partner. In the respective](#)
57 [complexes, the C-terminal residue of the ligand is referred to as P₀; subsequent residues towards the N-](#)
58 [terminus are termed P₋₁, P₋₂, and P₋₃ etc. Previous studies have revealed that P₀ and P₋₂ are most critical](#)
59 [for PDZ-ligand recognition \(Songyang 1997, Schultz 1998\).](#)

60 [PDZ domains are divided into at least three main classes on the basis of their amino acid preferences at](#)
61 [these two sites: class I PDZ domains recognize the motif S/T-X- \$\Phi\$ -COOH \(\$\Phi\$ is a hydrophobic residue](#)
62 [and X any amino acid\). Class II PDZ domains recognize the motif \$\Phi\$ -X- \$\Phi\$ -COOH, whereas class III](#)

hat gelöscht: ¶

hat formatiert: Schriftart: Fett

hat formatiert: Schriftart: Fett

hat formatiert: Schriftart: Fett

hat gelöscht: Post synaptic density protein (PSD95), *Drosophila* disc large tumour suppressor (Dlg1), and Zonula occludens-1 protein (ZO-1) domains termed

67 PDZ domains recognize the motif X-X-COOH. However, some PDZ domains do not fall into any of
68 these specific classes (Pawson 2007, Sheng 2001, Zhang 2003). The Dvl PDZ domains, for example,
69 recognize the internal sequence (KTXXXW) within the frizzled peptide 525(GKTLQSWRRFYH)536
70 ($K_D \sim 10 \mu\text{M}$) (Wong 2003, Chandanamali 2009).

71 [Due to their occurrence in important proteins, PDZ domains received early attention as drug targets,](#)
72 [nicely summarized in Christensen 2019.](#) There are several examples of [Dvl PDZ inhibitors of peptide](#)
73 [or peptidomimetic nature \(eg. Hammond 2006, Haugaard-Kedstrom 2021\), including peptide conjugates](#)
74 [\(eg. Qin 2021, Hegedus 2021\), and on an organic, small-molecule basis. The latter approach is](#)
75 [considered most beneficial in long term medical treatments of conditions like cancer or neurological](#)
76 [disorders.](#) NSC668036 (Shan 2005, Wang 2015) is a peptide-mimic compound which interferes with

hat gelöscht: small-molecule inhibitors of

77 Wnt signalling at the Dvl level. Based on a computational pharmacophore model of NCS668036,
78 additional compounds were later reported (Shan 2012). Known as first non-peptide inhibitor, the 1H-
79 indole-5-carboxylic acid derivative FJ9 (Fujii 2007) showed therapeutic potential. Further examples
80 including Sulindac (Lee 2009), 2-((3-(2-Phenylacetyl)amino)benzoyl)amino)benzoic acid (3289-8625,
81 also called CalBioChem(CBC)-322338) (Grandy 2009, Hori 2018), N-benzoyl-2-amino-benzoic acid
82 analogs (Hori 2018), phenoxyacetic acid analogs (Choi 2016), and Ethyl 5-hydroxy-1-(2-oxo-2-((2-
83 (piperidin-1-yl)ethyl)amino)ethyl)-1H-indole-2-carboxylate (KY-02327) (Kim 2016) have been
84 reported, with the latter showing the highest *in-vitro* affinity (8.3 μM) of all. Despite the existence of the
85 abovementioned inhibitors of Dvl PDZ, the development of tighter-binding, non-peptidic small-
86 compound modulators of the respective functions, binding with nanomolar affinity, is necessary and

hat gelöscht:

hat gelöscht:

87 remains challenging. [On this path, we explore optimal fits for the primary binding pocket by cycles of](#)
88 [chemical synthesis and X-ray crystallography and further avenues for systematically growing ligands](#)
89 [along the Dvl PDZ surface to provide SAR for the development of inhibitors in the low or medium](#)
90 [nanomolar range.](#) Nuclear magnetic resonance (NMR) spectroscopy was used to detect primary hits and
91 for follow-up secondary screening. The ability of NMR to detect weak intermolecular interactions (μM
92 $< K_D < \text{mM}$) make it an ideal screening tool for identifying and characterizing weakly binding fragments,
93 to be optimized subsequently by chemical modification in order to improve binding (Zartler 2006,
94 Shuker 1996, Zartler 2003). Besides NMR, the determination of X-ray crystal structures of selected

hat gelöscht: subsequent investigations

hat gelöscht: Here, n

100 complexes was fundamental for further design of new compound structures with improved binding. In
101 the first round of screening, a library constructed after computational docking of candidates into the
102 peptide binding site of the Dvl PDZ domains were investigated, followed by secondary screening
103 utilizing a library of 120 compounds containing rhodanine or pyrrolidine-2,5-dione moieties.
104

105 **RESULTS AND DISCUSSION**

106 **PDZ targeted library design**

107 The PDZ targeted library was designed to cover all PDZ domains with available structure. For this, all
108 X-ray and NMR derived PDZ structures were retrieved from the PDB, clustered, and 6 selected centroids
109 were subjected to the virtual screening routine. The area considered is shown in Figure 1A, with the blue
110 sphere indicating the geometrical centre. The clustering of the PDZ domains was performed according
111 to the shapes of their binding sites, rather than backbone conformation. This approach accounts for the
112 importance of surface complementarity of protein-small molecule interactions and the critical
113 contribution of van der Waals interactions to the binding free energy. On another hand, PDZ domains
114 have evolved to recognize a carboxyl group that is mostly derived from the C-terminus of natively
115 binding proteins. Finally, the fact that PDZ can recognize internal motifs (Hillier 1999), including
116 KTXXXW of Frizzled-7 recognised by Dvl PDZ (Wong 2003, Chandanamali 2009), raises the question
117 of what are key binding contributions with PDZ domains: negative charge, hydrogen bonding or shape
118 complementarity (Harris 2003). For this reason, tangible compounds were preselected to have extensive
119 hydrophobic contacts as well as chemical groups that mimic the carboxylic group.

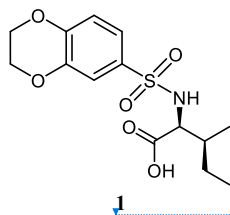
120 Virtual screening was performed with QXP, and the generated complexes were sequentially filtered with
121 a self-designed MultiFilter algorithm. From the resulting 1119 compounds a randomly selected set of
122 250 compounds was subjected to NMR validation.
123

124 **NMR Screening and development of compounds**

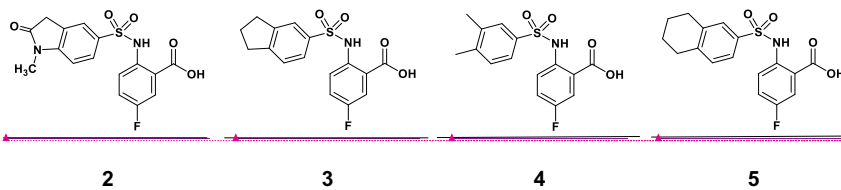
125 The results of virtual screening were checked experimentally by comparing 2D ^1H - ^{15}N HSQC
126 (Heteronuclear Single Quantum Correlation) spectra of Dvl-3 PDZ in the absence and presence of the
127 compound to elucidate ligand-induced changes of chemical shifts. Chemical shift perturbation

hat gelöscht: given

129 differences (ΔCSP , representing the average of the three strongest shifting cross peaks according to
 130 equation 1) were evaluated in cases where the residues responding strongest are inside the area defined
 131 by Figure 1A. The responses were classified into: (i) inactive compounds ($\Delta\text{CSP} < 0.02$); (ii) very weak
 132 interactions ($0.02 \leq \Delta\text{CSP} \leq 0.05$); (iii) weak interactions ($0.05 < \Delta\text{CSP} \leq 0.1$); (iv) intermediate
 133 interactions ($0.1 < \Delta\text{CSP} \leq 0.2$); (v): strong interactions ($0.2 < \Delta\text{CSP} \leq 0.5$) and (vi) very strong
 134 interactions ($\Delta\text{CSP} > 0.5$). In most cases, the signals of residues S263, V287 and R320 (Figure 1A)
 135 within the conserved binding site were most strongly perturbed (Supporting Information Figure S2).
 136 With the ΔCSP of 0.12 ppm, the isoleucine-derived compound **1** ((2,3-dihydrobenzo[b][1,4]dioxin-6-
 137 yl)sulfonyl)-L-isoleucine containing a sulfonamide moiety was detected initially as one of the best “hits”
 138 according to chemical shift changes. The sulfonamide is a well-known moiety in drug discovery
 139 (Mathvink 1999, Wu 1999, Sleight 1998 O’Brien 2000, Tellew 2003).



141
 142 Upon NMR titration experiments for compound **1** (Supporting Information Figure S2) with Dvl-3 PDZ,
 143 the largest chemical shift perturbations were observed for S263 in strand βB and R320 in helix αB of
 144 Dvl-3 PDZ, confirming the conserved binding site.
 145



147 **Scheme 1:** Compounds **2**, **3**, **4**, **5**
 148 By comparing the binding of several sulfonamide compounds in a secondary screening event and mak-
 149 ing use of our in-house library, four new compounds (**2**, **3**, **4**, **5**) that induced chemical shift perturbations
 150 larger than 0.2 ppm were found (for binding constants see Table 1) and considered further as reasonably

hat gelöscht: , usually S263, V287 and R320

hat gelöscht: s

hat gelöscht: for compounds that cause shifts of at least three N-H cross-peaks. T

hat gelöscht: esponding r

hat gelöscht: all

hat gelöscht: were

hat gelöscht: 1

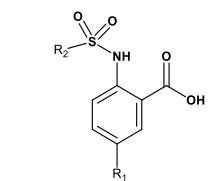
Feldfunktion geändert

Feldfunktion geändert

Feldfunktion geändert

Feldfunktion geändert

159 strong binders. The similarity of the structures led us to define Scheme 2 as a scaffold for further refine-
160 ments. Sulfonamides were considered more drug-like, and hence followed up at higher priority than
161 other hits. We realised that our four new compounds had different moieties at R₂ in combination with a
162 small R₁ (fluorine). A decrease of binding was observed with decreasing size of R₂.



163 **Scheme 2:** Basic fragment for further synthesis

164 In order to assess the importance of the aryl group at R₂ for complex formation, it was replaced by a
165 methyl group as substituent to yield compound **6**, which showed a drastic decrease of binding (Table 1).
166 Compounds **3**, **4**, and **5** did not distinguish between the Dvl-3 PDZ and Dvl-1 PDZ. In order to obtain
167 detailed insight into the binding mode of these compounds, crystal structures of Dvl-3 PDZ in complex
168 with compounds **3**, **5** and **6** were determined (Figure 1). For compound **3** the crystal structure revealed
169 two complexes within the crystallographic asymmetric unit (AU) at 1.43 Å resolution. Both show the
170 anthranilic acid with the attached fluorine pointing into the hydrophobic binding pocket (Figure 1B and
171 Supporting Information Figure S3A), while the carboxyl group forms a hydrogen-bond network with
172 amide residues of the carboxylate binding loop, in particular strand βB (Figure 1B) and specifically with
173 residues I262, G261 and L260. The two sulfonamide oxygen atoms form hydrogen bonds with R320
174 and H324 (weak) of helix αB for only one complex in the AU. The aromatic aryl group
175 (tetrahydronaphthalene) attached to the sulfonamide is involved in hydrophobic interactions with F259
176 (Supporting Information Figure S3B). The 1.6-Å complex structure with compound **5** (4 molecules per
177 AU) exhibits a comparable binding mode as found for compound **3** with a hydrogen-bond network
178 involving the carboxyl group and the amides of I262, G261, L260, and of the sulfonamide to H324
179 (Figure 1C). No hydrogen bond was observed to R320 in all four molecules of the AU, but small
180 variations of the aryl moiety relative to F259 (Supporting Information Figure S3C). The crystals of the
181 complex with **6** show two molecules in the AU (Figure 1D). The sulfonamide is bound by H324 in both

hat gelöscht: ¶

Seitenumbruch

hat gelöscht: 1A

hat gelöscht: 1A

hat gelöscht: 1B

hat gelöscht: 1C

189 complexes (Supporting Information Figure S3D). However, compound **6** bound only in the mM range
 190 as compared to **3** and **5**, which obviously results from the missing aromatic rings.

191

hat gelöscht:Seitenumbruch.....

	ID	R ₁	R ₂	(K _D , μM) Dvl-3PDZ	(K _D , μM) Dvl-1 PDZ
	2	F		nd	237.6 ± 38.5 ^{NMR}
	3	F		80.6 ± 6.1 ^{NMR}	112.7 ± 25.9 ^{NMR}
	4	F		83.9 ± 7.8 ^{NMR}	114.4 ± 9.8 ^{NMR}
	5	F		140.6 ± 14.1 ^{NMR}	160.1 ± 14.6 ^{NMR}
	6	F	CH ₃	> 1000 ^{ITC}	-
	7	Br		20.6 ± 2.4 ^{NMR}	18.2 ± 2.4 ^{NMR}
	8	CF ₃		17.4 ± 0.5 ^{ITC}	24.5 ± 1.5 ^{ITC}
	9	Cl		41.1 ± 3.1 ^{NMR}	45.6 ± 4.5 ^{NMR}
	10	CH ₃		62.5 ± 4.7 ^{NMR}	60.5 ± 5.3 ^{NMR}
	11	Br		13.8 ^{ITC}	119.9 ^{ITC}
	12	Br		58.5 ^{ITC}	nd
	13	Br		7.2 ^{ITC}	213.2 ^{ITC}
	14	Br		58.1 ± 2.1 ^{ITC}	nd
	15	CF ₃		52.9 ± 1.7 ^{ITC}	nd
	16	CF ₃		59.1 ± 1.5 ^{ITC}	nd
	17	CF ₃		49.5 ^{ITC}	nd
	18	CH ₃		9.4 ± 0.6 ^{ITC}	2.4 ± 0.2 ^{ITC}
	19	CH ₃		21.8 ± 1.7 ^{ITC}	8.0 ± 0.5 ^{ITC}
	20	CH ₃		9.8 ± 0.3 ^{ITC}	4.7 ± 0.3 ^{ITC}
	21	CH ₃		12.5 ± 0.5 ^{ITC}	4.7 ± 0.2 ^{ITC}

192

193

194 **Table 1.** Binding constants K_D (μM) of Dvl-3 PDZ and Dvl-1 PDZ for compounds **3** – **21** derived by ITC or NMR if not
 195 specified. The K_D values determined by NMR are reported as means ± standard deviations of measurements evaluating shifts
 196 of cross peaks of at least six residues influenced upon binding of the ligand. The K_D values (1/K_D) determined by ITC were
 197 obtained as fits to a one-site binding model (n in the range of 0.95-1.2) with K_D errors obtained by ΔK_D/K_D².

198

hat formatiert: Tiefgestellt

hat gelöscht: d

hat formatiert: Tiefgestellt

hat formatiert: Tiefgestellt

hat gelöscht: 1.0

hat formatiert: Nicht Hervorheben

hat formatiert: Tiefgestellt, Nicht Hervorheben

hat formatiert: Nicht Hervorheben

hat gelöscht: the formula

hat formatiert: Nicht Hervorheben

hat formatiert: Tiefgestellt

hat formatiert: Tiefgestellt

hat formatiert: Hochgestellt

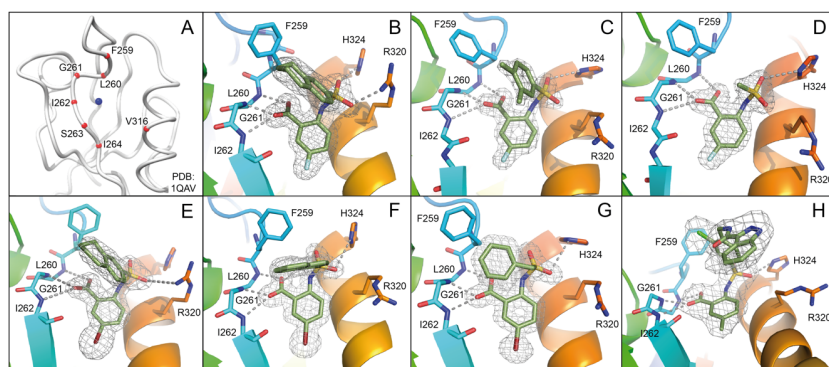
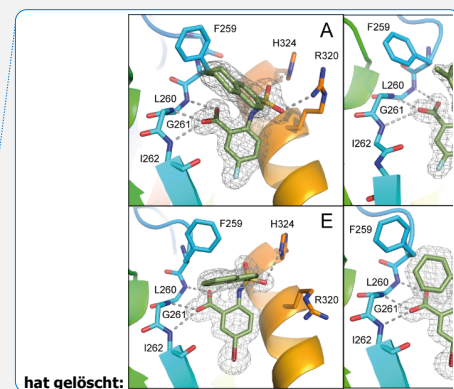


Figure 1: **A** Definition of PDZ binding site. The center of the binding site (blue sphere) is defined as the geometric center of Ca atoms (red spheres) of 7 residues (typed in red) defined by multiple sequence alignment. **B-H** Magnified views into crystal structures of various compounds bound to the Dvl-3 PDZ domain. The 2Fo-Fc electron density around the compounds is shown at 1 σ contour level, and the dotted lines indicate formed hydrogen bonds. In the bound compounds covalent bonds to carbon atoms are shown as green sticks. Important residues involved in compound binding are labelled and displayed in atom colours (carbons blue or dark yellow). **B-D** show compound **3**, **5** and **6** respectively. All compounds in **B-D** contain fluorine (light blue) in para position to the amine. **E-G** represents the bound compounds **7**, **11** and **12**, respectively. All have bromine (dark red) in para position to the amine. **H** shows compound **18** within the binding site. The accession codes of the structures **B-H** are 6ZBQ, 6ZBZ, 6ZC3, 6ZC4, 6ZC6, 6ZC7 and 6ZC8, respectively.

To further explore the importance of the fluorine site inside the hydrophobic pocket, substitutions by bromine, chlorine, methyl and trifluoromethyl were chosen. In fact, the methyl group has a similar vdW radius as the CF₃ group. Iodine was not considered a good candidate since it increases molecular weight substantially and the compounds may be chemically less stable, in particular in biological assays. Taking into account that compound **6** did not bind because of the missing aromatic ring at the R₂ position, our overall strategy was to increase the aromatic ring at R₂ while finding a good fit for R₁, keeping an eye on the molecular weight to enable further compound modifications that fulfil key properties as defined by Lipinski (Lipinski 2000, Lipinski 1997). Our preference to continue exploration at the R₁ position of the aromatic ring in Scheme 1 was inspired by the absence of hits with other substitutions in the secondary screening event and the initial X-ray structures that showed a hydrophobic pocket available for substituents in this position while other sites at the aromatic ring would include steric hindrance. Therefore, compounds **7-17** were obtained and were classified in three different groups to derive structure activity relationships (SAR). The compounds **7-10** in group 1 contain different R₁ (Br, CF₃, Cl, CH₃) but the same moiety (tetrahydronaphthalene) at R₂. As expected, binding could be further improved by displacement of the fluorine with elements exhibiting larger van der Waals (vdW) radii.



hat formatiert: Schriftart: Nicht Fett

hat formatiert: Schriftart: Fett

hat gelöscht: A

hat gelöscht: C

hat gelöscht: A

hat gelöscht: C

hat gelöscht: D

hat gelöscht: F

hat formatiert: Schriftart: Fett

hat formatiert: Schriftart: Fett

hat formatiert: Nicht Hervorheben

hat formatiert: Nicht Hervorheben

hat gelöscht: accordingly

hat gelöscht: ¶

hat gelöscht: keeping

hat formatiert: Nicht Hochgestellt/ Tiefgestellt

hat gelöscht: as small as possible (preferably CH₃) to

hat gelöscht: only

241 Indeed, the K_D decreased stepwise and the best fit was observed for compound **8** containing a
242 trifluoromethyl group ($K_D = 17.4 \mu\text{M}$ for Dvl-3 PDZ and $24.5 \mu\text{M}$ for Dvl-1 PDZ). The different
243 substituents at the R_2 position contribute to an increased binding affinity in the following order: $F < \text{Cl}$
244 $< \text{Br} < \text{CF}_3$ (compound **3** $< \mathbf{9} < \mathbf{7} < \mathbf{8}$, respectively). Compound **10** with a methyl group at the R_2 position
245 showed only marginally improved binding, although the methyl group has a similar vdW radius as the
246 CF_3 group of compound **8**. The difference in binding results most likely from their different
247 hydrophobicity.

248 The 1.85-Å crystal structure of the Dvl-3 PDZ domain with compound **7** ($K_D = 20.6 \mu\text{M}$ for Dvl-3 PDZ
249 and $18.2 \mu\text{M}$ for Dvl-1 PDZ) showed an identical hydrogen-bond network involving the amide groups
250 of residues I262, G261 and L260 of the carboxyl binding loop as seen for all other complex structures
251 reported here (Figure [1E](#)). Only one hydrogen bond between the sulfonamide and R320 was found in
252 addition for one of the two Dvl-3 PDZ molecules per AU. H324 of Dvl-3 PDZ was not addressed by the
253 sulfonamide as seen previously. The bromine at position R_1 points into the hydrophobic pocket, similar
254 as the fluorine in the complex structure with compound **3**. The two complexes in the AU show significant
255 variations in the positions of the tetrahydronaphthalene rings as well as for the side chain of F259 and
256 R320 (Supporting Information Figure S3E).

257 Following the analysis of the complex involving compound **7**, the binding characteristics of the group-
258 2 compounds (**11-14**) were investigated. They contain bromine as R_1 and different substituents at the R_2
259 position to assess the importance of π - π stacking interactions involving F259. K_D values of $7.2 \mu\text{M}$ for
260 compound **13** and $13.8 \mu\text{M}$ for compound **11** were found with respect to the interaction with Dvl-3 PDZ.
261 Crystal structures of Dvl-3 PDZ in complex with compound **11** (1.58 Å resolution, 1 molecule per AU)
262 and **12** (1.48 Å, 2 molecules per AU) revealed very similar binding as observed in the crystal structures
263 with compounds **3** and **7**. The aromatic rings at R_2 show hydrophobic interactions to F259, but not a
264 classical π - π stacking as expected. Nevertheless, the tighter binding of compound **11** could be explained
265 by the larger aromatic substituent at the R_2 position compared to compound **12**. Both complex structures
266 show also non-specifically bound ligands in crystal contacts (Supporting Information Figure S3H,
267 Supporting Information Tables S2 and S3). The additional ligand molecules in both complex structures
268 can be explained as a crystallographic artefact, which is verified with ITC experiments that indicate 1:1

hat gelöscht: 2

hat gelöscht: 2

hat gelöscht: 1D

272 stoichiometries in both cases (Figure S5). With respect to the selectivity of the tested compounds we
273 observed a 6 to 30-fold stronger binding of compounds **7**, **9**, **11** and **13** to Dvl-3 PDZ as compared to
274 Dvl-1 PDZ. These differences are related to the different sequences at the end of α B. Most importantly,
275 H324 is replaced by a serine residue in the Dvl-1 PDZ domain.

276 The group-3 compounds (**15-17**) contain a trifluoromethyl at position R_1 and were tested to investigate
277 a cooperative role of this moiety with various substituents at position R_2 . All compounds bind weaker
278 to Dvl-1 and Dvl-3 than compound **8** which contains tetrahydronaphthalene at the R_1 position, revealing
279 its important role in the interaction.

280

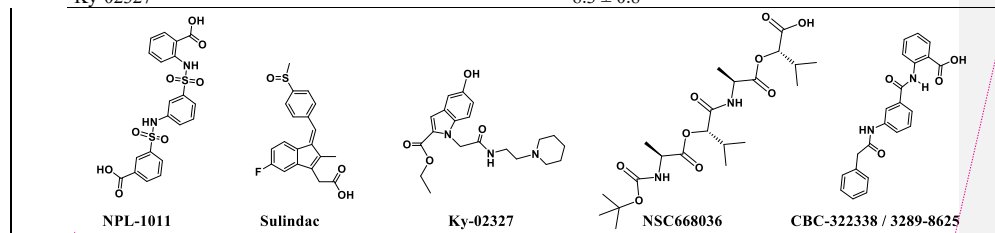
281 **Further modifications towards higher affinity and reduced toxicity**

282 Possible cytotoxic effects of compounds **3**, **7**, **8**, **9**, and **10** were evaluated in cell viability assays using
283 HEK293 cells (Supporting Information Figure S4). These compounds were selected due to different
284 substituents at the R_1 , including halogens. Cell viability was measured 24h after treatment with the
285 individual compounds, and half maximal inhibitory concentrations (EC_{50}) were calculated for each
286 compound. The compounds exhibited EC_{50} values in the range of 61-131 μ M (Supporting Information
287 Figure S4A). Compounds **3** and **10** that contained fluorine or methyl group substituents at R_2 ,
288 respectively, were the least toxic, while compound **7**, containing bromine, was the most toxic. The
289 results from crystallography, modelling studies and of the cell proliferation assays led us to further
290 investigate compounds **18-21** that contain a methyl group at the R_1 position and different substituents
291 as R_2 . In this way, we aimed to develop both potent and less toxic, cell permeable inhibitors. All
292 compounds showed strong interactions as indicated by chemical shift perturbation values between 0.30
293 to 0.34 ppm (Supporting Information Table S1). The binding constants were evaluated by ITC whereby
294 compound **18** ($K_D = 9.4 \mu$ M for Dvl-3 PDZ and 2.4μ M for Dvl-1 PDZ) appeared to be most potent.
295 Compound **18** contains a pyrazole ring which is considered as an important biologically active
296 heterocyclic moiety (Lv 2010). Compounds **20** ($K_D = 9.8 \mu$ M for Dvl-3 PDZ and 4.7μ M for Dvl-1 PDZ)
297 and **21** ($K_D = 12.5 \mu$ M for Dvl-3 PDZ and 4.7μ M for Dvl-1 PDZ) contain pyrrole rings. Their binding
298 constants almost have the same value despite the different substituents (bromine or chlorine) at the
299 pyrrole rings. The binding of compounds **18-21** to both Dvl PDZ domains is mainly enthalpy-driven as

300 indicated in Table 2, with a slightly stronger effect for Dvl-1 PDZ than for Dvl-3 PDZ. To our surprise,
 301 the crystal structure of Dvl-3 PDZ in complex with compound **18** shows the pyrazole substituent in the
 302 R₂ position orientated away from the binding pocket. Instead, a π - π stacking interaction with F259 was
 303 observed (Supporting Information Figure S3I). Cytotoxicity of **18-21** was determined *via* MTT assays
 304 (Mosmann 1983) that displayed viability up to concentrations above 150 μ M (Supporting Information
 305 Figure S4B).

306

Compound	Dvl-3 PDZ				Dvl-1 PDZ			
	K _D (μ M)	Δ H (kcal/mol)	T Δ S (kcal/mol)	Δ G (kcal/mol)	K _D (μ M)	Δ H (kcal/mol)	T Δ S (kcal/mol)	Δ G (kcal/mol)
18	9.4 \pm 0.6	-8.0	-1.2	-6.8	2.4 \pm 0.2	-12.2	-4.7	-7.5
19	21.0 \pm 1.7	-5.9	0.4	-5.5	8.0 \pm 0.5	-7.3	-0.3	-7.0
20	9.8 \pm 0.3	-10.4	-3.6	-6.8	4.7 \pm 0.3	-9.4	-2.2	-7.2
21	12.5 \pm 0.5	-5.9	0.7	-6.8	4.7 \pm 0.2	-8.5	-1.5	-7.0
NPL-1011	79.7 \pm 53.3							
Sulindac	8.3 \pm 2.5							
CBC-322338/ 3289-8625	> 400 μ M							
NSC668036	> 400 μ M							
Ky-02327					8.3 \pm 0.8 ^{16g}			



310

311 **Table 2:** Isothermal titration calorimetric data for the reaction between Dvl-3 PDZ, Dvl-1 PDZ and our compounds **18**, **19**, **20**
 312 and **21** respectively. Compounds NPL-1011 (Hori 2018), and Sulindac (Lee 2009), CBC-322338/3289-8625 (Grandy 2009,
 313 Hori 2018), and NSC668036 (Shan 2005), for more thermodynamic parameters see Supporting Information Figure S7. For Ky-
 314 02327 the value from literature is included.

315

316 Comparison to reported Dvl PDZ-binding molecules

317 Our compounds bind to Dvl-3 with a K_D better than 10 μ M, and slightly tighter to Dvl-1, see Table 2,
 318 with **18** showing a K_D of 2.4 μ M and chemical shift changes indicating binding to the canonical binding
 319 site (Figure 1A). For comparison, four compounds of those shown in Supporting Information Figure S6
 320 were assayed by ITC (Supporting Information Figure S7) regarding their affinity to Dvl-3 PDZ. Ky-
 321 02327 was already determined to bind with a K_D of 8.3 \pm 0.8 μ M (Kim 2016) to Dvl-1 PDZ. Our first
 322 interest was oriented towards sulfonamides. Hori et al (Hori 2018) have recently reported 3-(3-(2-

hat gelöscht: d
 hat formatiert: Tiefgestellt
 hat gelöscht: d
 hat formatiert: Tiefgestellt

Feldfunktion geändert

hat formatiert: Tiefgestellt
 hat gelöscht: d
 hat gelöscht: Kd
 hat formatiert: Tiefgestellt
 hat gelöscht: Supporting Information
 hat gelöscht: S8
 hat gelöscht: he ones
 hat formatiert: Tiefgestellt
 hat gelöscht: d

331 carboxyphenyl)sulfamoyl]phenyl)sulfamoyl]benzoic acid (NPL-1011) binding to Dvl-1 PDZ via the
332 detection of chemical shift changes, and further sulfonamide compounds that showed smaller effects,
333 indicating weaker binding. We examined the binding constant of NPL-1011 which possesses two
334 sulfonamide moieties by ITC and found a value of $79.7 \pm 53.3 \mu\text{M}$, see Table 2. For further comparisons,
335 we assayed also CBC-322338/3289-8625, Sulindac and NSC668036 by ITC. Surprisingly, CBC-
336 322338/3289-8625 showed very low affinity, with a K_D above $400 \mu\text{M}$ in our ITC assay, in line with
337 the value found by Hori et al (Hori 2018) ($954 \pm 403 \mu\text{M}$). We also applied an NMR shift assay (Figure
338 S8), yielding a ΔCSP around 0.1. Based on NMR and ITC studies, the binding affinity of CBC-
339 322338/3289-8625 to DVL-3 seems to be less than 50 micromolar, comparing the CSPs from the NMR
340 assay with those of our other compounds listed in Table S1 and the respective binding constants in Table
341 1, and considering also the weak heat development in our ITC assay, which was larger than the originally
342 reported value (10.6 ± 1.7) (Grandy 2009) that was obtained with a different method. Concerning non-
343 sulfonamide compounds, a K_D of $8.3 \pm 2.5 \mu\text{M}$ was detected for Sulindac, while NSC668036 (Shan
344 2005) did not show high-affinity binding. These results are largely in agreement with literature. In all
345 cases, compounds were tested for purity after K_D measurements (see Supporting Information Figures
346 S9A-D).

347 Selectivity testing using a set of selected PDZ domains

349 Compounds **18**, **20** and **21** were tested towards other PDZ domains for selectivity. The set included
350 PSD95-PDZ 2 and 3, Shank-3, α -syntrophin, and AF-6 PDZ. According to the determined chemical
351 shift perturbations (Supporting Information Table S4), our compounds show no or very weak
352 interactions with the selected PDZ domains ($0.05 < \Delta\text{CSP} \leq 0.1$) ppm. These findings led to the
353 conclusion that our compounds show considerable selectivity towards Dvl PDZ domains. This
354 selectivity might be due to a unique feature of Dvl PDZ where R320 (Dvl-3 PDZ) or R322 (Dvl-1 PDZ)
355 are crucial for interactions, explaining selectivity with respect to other PDZ domains. In addition, the
356 large hydrophobic cavity for the side chain of the C-terminal residue of the interacting peptide is
357 occupied by a large moiety in case of compounds **18**, **20** and **21** which might not be accommodated in
358 most other PDZ domains.

359

- hat gelöscht: d
- hat gelöscht: (assumed to be the threshold for our ITC assay), which was larger than the originally reported value (10.6 ± 1.7) (Grandy 2009) and closer to
- hat formatiert: Tiefgestellt
- hat formatiert: Schriftart: Symbol
- hat gelöscht: well
- hat formatiert: below
- hat formatiert: Schriftart: 11 Pt.
- hat gelöscht: ,
- hat formatiert: Schriftart: 11 Pt.
- hat formatiert: Schriftart: 11 Pt.
- hat gelöscht:
- hat formatiert: Schriftart: 11 Pt.
- hat gelöscht: and c
- hat formatiert: Schriftart: 11 Pt.
- hat gelöscht: ,
- hat gelöscht: Concerning
- hat formatiert: Tiefgestellt
- hat gelöscht: d
- hat formatiert: Schriftart: 11 Pt.
- hat gelöscht: Kd
- hat formatiert: Tiefgestellt

373 **Dvl inhibitors antagonize canonical Wnt signalling and Wnt-related properties of cancer cells**

374 Taking advantage of a lentivirus that encodes GFP in a β -catenin/TCF-dependent fashion (TOP-GFP,
375 SABiosciences), a stable HEK293 reporter cell line was established to evaluate the inhibitory effect of
376 compounds **18**, **20** and **21** on canonical Wnt signalling activity. TOP-GFP expression in this cell line
377 was induced by the ligand Wnt3a, which directly activates the Frizzled-Dishevelled complex and
378 protects β -catenin from degradation by the destruction complex (Figure 2A). Remarkably, all three
379 compounds inhibited Wnt signalling induced by Wnt3a in a dose-dependent manner (Figure 2B),
380 yielding IC_{50} values between 50-80 μ M.

Formatiert: Zeilenabstand: Doppelt, Tabstopps: Nicht an 2,91 cm

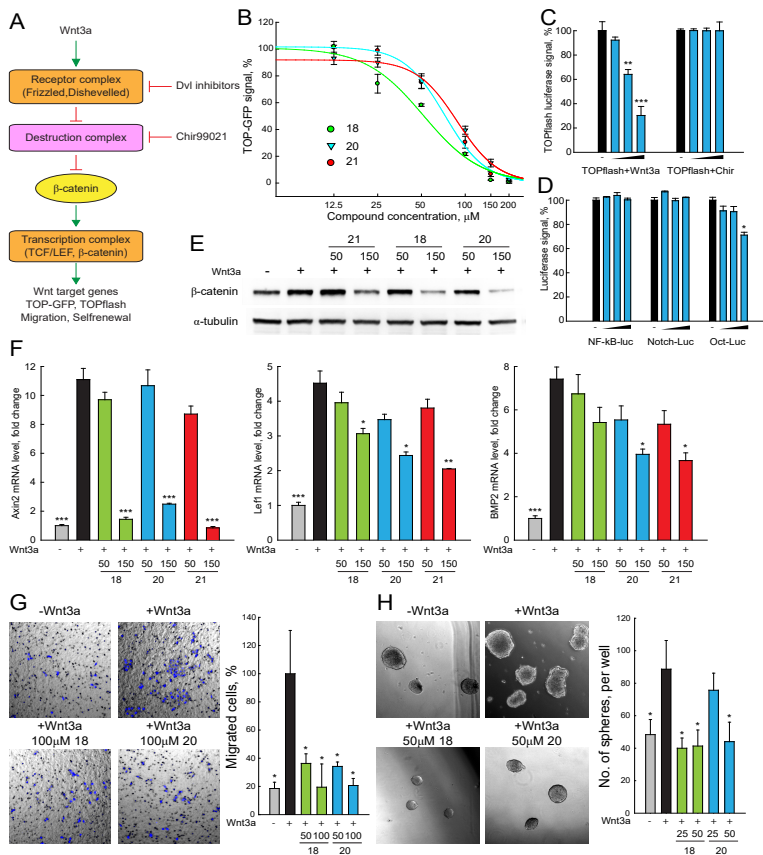


Figure 2

hat formatiert: Schriftart: (Standard) Arial, 10 Pt.

Figure 2. DVL inhibitors antagonize Wnt signalling and Wnt related properties of cancer cells induced by Wnt3a. **A.** Scheme of Wnt signalling pathway. Important components of the Wnt signalling pathway are schematically presented. Wnt3a treatment increases the transcription of Wnt targets, enhances signals of TOP-GFP and TOPflash assays, and promotes Wnt related biological properties of cancer cells. **B.** TOP-GFP reporter assays were performed with HEK293 reporter cell line. Compound **18**, **20** and **21** inhibited Wnt3a induced Wnt activation in dose-dependent manner with IC_{50} of 50~75 μ M. **C.&D.** TOPflash assays stimulated with Chir99021 and reporter assays of other pathway were used to evaluate the specificity of compound **20**. Compound **20** specifically inhibited Wnt3a induced Wnt activation, and had no or mild effect on Chir99021 induced Wnt activation and other signalling pathways including NF- κ B, Notch and Oct4. **E.** β -Catenin protein levels were detected with Western blotting in HeLa cells. Compound **18**, **20** and **21** (150 μ M) inhibited accumulation of β -catenin in HeLa cells treated with Wnt3a. **F.** The mRNA levels of Wnt target genes (Axin2, Lef1 and Bmp2) in HeLa cells were measured with quantitative real-time PCR. Compounds **18**, **20** and **21** (150 μ M) reduced the transcription of Wnt target genes that are enhanced by Wnt3a treatment in HeLa cells. **G.** Cell migration of SW480 cells after Wnt3a treatment was assessed by transwell assays. Compounds **18** and **20** (50~100 μ M) reduced the migration of SW480 cells enhanced by Wnt3a. **H.** SW480 cells were cultured in serum-free non-adherent condition to evaluate the self-renewal property enhanced by Wnt3a treatment. Compound **18** and **20** (25~50 μ M) reduced sphere formation of SW480 cells that was enhanced by Wnt3a treatment. [For all tests, three independent biological replicates were performed and error bars represent standard deviations. P-values were calculated from T-test. *; P < 0.05; **; P < 0.01; ***; P < 0.001.](#)

hat gelöscht: For all tests, three independent biological replicates were performed. Error bars represent standard deviations, and P-values were calculated from T-test. *; P < 0.05; **; P < 0.01; ***; P < 0.001.

404

405 To further evaluate the specificity of our Dvl inhibitors, the conventional TOPflash (Molenaar 1996)
406 and other luciferase reporter assays were performed. In HeLa cells, **20** inhibited TOP-luciferase signals
407 stimulated by Wnt3a but not by CHIR99021 (Sineva 2010), a compound that activates Wnt signalling
408 downstream of Dvl (Figure 2A, C). Compound **20** had no significant inhibitory effects in reporter assays
409 that measure the activity of other signalling systems, e.g., NF- κ B-luciferase stimulated by recombinant
410 TNF α , Notch-luciferase stimulated by the overexpression of the Notch intracellular domain, or the Oct-
411 luciferase assay that is stimulated by overexpression of Oct4 (SABiosciences, Figure 2D). These results
412 strongly indicate that **20** is specific for canonical Wnt signalling at the upstream level.

413 Increased β -catenin protein level is a hallmark of active Wnt signalling (Kishida 1999). Once β -catenin
414 is accumulated in the cytoplasm, it can translocate into the nucleus and activate the transcription of Wnt
415 target genes by interacting with transcription factors of the TCF/LEF family (Figure 2A) (Behrens
416 1996). In HeLa cells, all three Dvl inhibitors blocked the increase of production of β -catenin by Wnt3a
417 in dose-dependent manners, as seen by Western blotting (Figure 2E). Increased mRNA levels of the
418 Wnt target genes Axin2, Lef1 and Bmp2 (Riese 1997, Jho 2002, Lewis 2010) were induced by Wnt3a
419 treatment, as measured by qRT-PCR, and these increases were reduced by compounds **18**, **20** and **21**
420 (Figure 2F). These results demonstrate that compounds **18**, **20** and **21** inhibit Wnt signalling as indicated
421 by reduced accumulation of β -catenin and low expression of typical Wnt target genes.

422 Canonical Wnt signalling contributes to cancer progression by inducing high motility and invasion of
423 cancer cells while retaining the self-renewal property of cancer initiating cells (Fritzmann 2009, Sack
424 2011, Vermeulen 2010, Malanchi 2008). In particular, cancer initiating cells are propagated and
425 enriched in non-adherent sphere culture, demonstrating the self-renewal capacity of the stem cells
426 (Kanwar 2010, Fan 2011). To investigate the potential value of the Dvl inhibitors for interfering with
427 these Wnt-related properties of cancer cells, the subline SW480WL was derived from the SW480 colon
428 cancer cell line, which exhibits a low level of endogenous Wnt activity (Fang 2012). The cell migration
429 and self-renewal properties of SW480WL cells were enhanced by Wnt3a treatment, as revealed by
430 transwell and sphere formation assays (Figure 2G, H). Compounds **18** and **20** prevented increased cell

431 migration and sphere formation. These results indicate that our Dvl inhibitors may be developed into
432 lead compounds that interfere with Wnt signalling.

433

434 **CONCLUSIONS**

435 In the present work, small molecules that bind to Dvl PDZ in the one-digit micromolar range with
436 considerable selectivity have been developed by an extensive structure-based design approach. With
437 regards to the affinity determined by ITC, compound **18** binds to Dvl-1 and Dvl-3 in vitro with K_d values
438 of 2.4 and 9.4, respectively, comparing very well with known ligands. X-ray structures of Dvl-3 PDZ
439 complexes with selected compounds provided insight into crucial interactions and served as the basis
440 for the design of tight binding compounds with reduced toxicity. The structural investigations revealed
441 that these compounds form hydrogen bonds with the amide groups of residues L260, G261 and I262 in
442 the PDZ-domain loop and the side chains of residues H324 and R320. Finally, the chosen methodology,
443 virtual screening followed by a two-stage NMR based screening, X-ray crystallography, and chemical
444 synthesis is an excellent path towards bioactive interaction partners. Our best compounds effectively
445 inhibited the canonical Wnt signalling pathway in a selective manner and could be developed for further
446 studies.

447

448 **Experimental Section**

449 **Clustering binding sites and selection of representative PDZ domains**

450 Three-dimensional structures of PDZ domains were retrieved from the PDB (Berman 2000). At the time
451 of the study from a total of 266 PDB files, 126 were NMR solution structures and 140 derived from X-
452 ray diffraction studies. The structures belong to 163 PDZ domains of 117 different proteins from 11
453 organisms. Files which contain more than one 3D conformation for a domain (up to 50 for NMR-derived
454 data) were split into separate structures and considered independently. The total number of unique 3D
455 structures was 2,708.

456 Amino acid sequences of PDZ domains were aligned using Clustal Omega software (Sievers 2011).
457 Based on the alignment, for each structure, residues which form the binding site (strand β B and helix
458 α B) were determined (Supporting Information Figure S8). The centre of the binding site was defined as

hat formatiert: Tiefgestellt

hat gelöscht: d

460 a geometric centre of C α atoms of 7 residues (6 residues from the β B strand and the second residue from
461 the α B helix). Such bias toward the β B strand was made to cover sites occupied by residues in -1 and -
462 3 positions.

463 The triangulated solvent accessible surface for each PDZ structure was built using MSMS software
464 (Sanner 1996) with a spherical probe radius of 1.4 Å and vertex density 10 Å⁻¹. The largest connected
465 set of surface vertices within 9 Å from the centre of the binding site was used to construct shape-based
466 numerical descriptors. The descriptors are 508-dimensional vectors of non-negative integer numbers
467 and were built using a shape distributions approach (Osada 2002). In total 10 (Pawson 2007) vertex
468 triplets were selected randomly, each forming a triangle. Triangles which had a side longer than 16 Å
469 were discarded. Triangle sides were distributed into 16 length bins, each 1 Å wide, covering lengths
470 from 0 to 16 Å. A combination of three sorted side lengths, each belonging to one of 16 distance bins,
471 defines one of 508 categories of the triangles. The number of triangles of each category was calculated,
472 resulting in a 508-dimensional vector which is used as a numerical descriptor of the binding pocket
473 shape. For further operations with descriptors, Euclidian metric was introduced. Shape descriptors were
474 distributed into 6 clusters using k-means algorithm (Jain 1988). For each cluster, a centroid structure
475 was defined as the one, whose descriptor is the closest to mean descriptor for the cluster. The centroid
476 structures (2O2T#B.pdb, 1VA8#3.pdb, 2DLU#01.pdb, 1UHP#8.pdb, 2OS6#8.pdb, 3LNX#A.pdb) were
477 used for docking.

478

479 **PDZ targeted library design**

480 Screening collection by Enamine Ltd. (Chuprina 2010) containing a total of 1,195,395 drug-like
481 compounds was used as the primary source of small molecules. Natural ligand of PDZ is the C-terminus
482 of a peptide with carboxylic group making extensive hydrogen bond network with the “ΦGΦ” motif.
483 Since the carboxyl provides either of negative charge and hydrogen bond acceptor, we want our ligands
484 to retain at least one of these features. Therefore, we pre-filtered the stock library to bear chemical
485 groups which have negatively charged and/or hydrogen bond acceptor functionality. In total 65,288
486 compounds were selected for the virtual screening study. The selected 6 centroids of PDZ domains and
487 the prepared compound set were subjected to high-throughput docking using the QXP/Flo software

488 (McMartin 1997). Complexes were generated with 100 steps of sdock + routine, and 10 conformations
489 per complex were saved.

490 Processing of docking poses started with filtering by contact term *Cntc* from the QXP/Flo scoring
491 function. Entries with *Cntc* < 45 were discarded, which removed complexes with weak geometries of
492 bound ligands. The remained filtering was performed with the in-house MultiFilter program that allows
493 flexible geometry-based filtering. We applied two algorithms, *nearest-atom* filter and *hydrogen-bond*
494 filter. The former filters complexes by distance from a given protein atom to the nearest heavy ligand
495 atom, while in the latter, filtering is based upon the number of hydrogen bonds calculated for a given
496 complex geometry. With the *nearest-atom* routine we selected compounds that filled the P₀ pocket and
497 sterically mimicked binding of a peptide carboxylic group. Peptide group hydrogens of the “ΦGΦ” motif
498 and atoms forming the hydrophobic pocket were used for that. With the *hydrogen-bond* filter we selected
499 compounds that formed extensive hydrogen bonding with the PDZ domain. Both these properties might
500 have larger impact on binding rather than negative charge (Harris 2003). Details on atoms used for
501 filtering and thresholds for *hydrogen-bond* filtering, as well as the resulting number of compounds, are
502 provided in Supporting Information Table S5. Compounds from complexes which passed through these
503 filters were incorporated into a targeted library for the PDZ-domain family. The final library contained
504 1119 compounds in total.

505

506 **Screening of compounds**

507 Two-dimensional ¹H-¹⁵N HSQC spectra were used to screen a library of 212 compounds designed by
508 the company Enamine for PDZ domains. 50 μM of ¹⁵N-labeled protein samples were prepared in a 20
509 mM sodium phosphate buffer, containing 50 mM sodium chloride, 0.02% (w/v) NaN₃, at pH 7.4. Stock
510 solutions of small molecules were prepared in DMSO-*d*₆ at a concentration of 160 mM. A ¹H-¹⁵N HSQC
511 spectrum of Dvl PDZ was acquired at 300 K with 5% DMSO-*d*₆ in the absence of ligand as reference
512 spectrum. Mixtures of 16 compounds were added to ¹⁵N-labeled Dvl PDZ at 8-fold molar excess each.
513 The final concentration of DMSO-*d*₆ in the protein-ligand solutions was 5%. Spectra were acquired
514 with 8 scans and 256 points in the indirect dimension. Compound binding was deduced if the resonance
515 position of a cross-peak was significantly shifted compared to the reference spectrum. The active

516 compound was obtained through successive deconvolution. Experiments were recorded on a Bruker
517 DRX600 spectrometer equipped with a triple-resonance cryoprobe. The preparation of samples was
518 done automatically by a Tecan Genesis RSP 150 pipetting robot. Spectra were analysed using the
519 programs TOPSPIN and SPARKY.⁴⁷

520

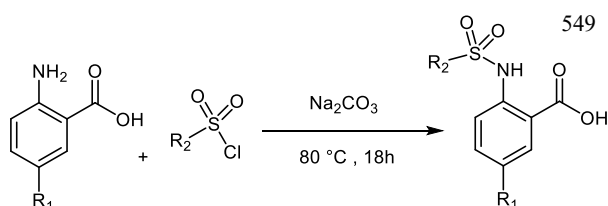
521 **Synthesis of compounds**

522 All reagents and starting materials were purchased from Sigma-Aldrich Chemie GmbH, ABCR GmbH
523 & Co.KG, alfa Aesar GmbH & Co.KG or Acros Organics and used without further purification. All air
524 or moisture-sensitive reactions were carried out under dry nitrogen using standard Schlenk techniques.
525 Solvents were removed by evaporation on a Heidolph Laborota 4000 with vacuum provided by a PC
526 3001 Vaccubrand pump. Thin-layer chromatography (TLC) was performed on plastic-backed plates pre-
527 coated with silica gel 60 F₂₅₄ (0.2 mm). Visualization was achieved under an ultraviolet (UV) lamp (254
528 and 366 nm). Flash chromatography was performed using J.T Baker silica gel 60 (30-63 µm). Analytical
529 high-performance liquid chromatography (HPLC) was performed on a Shimadzu LC-20 (degasser
530 DGU-20A3, controller CBM-20A, autosampler SIL-20A) with a DAD-UV detector (SPD-M20A),
531 using a reverse-phase C18 column (Nucleodur 100-5, 5 µM, 250 mm x 4 mm, Macherey-Nagel, Düren,
532 Germany). Separation of compounds by preparative HPLC was performed on a Shimadzu LC-8A
533 system equipped with a UV detector (SPD-M20A), using a semi-preparative C18 column (Nucleodur
534 100-5, 5 µM, 250 mm x 10 mm, Macherey-Nagel) or preparative C18 column (Nucleodur 100-5, 5 µM,
535 250 mm x 21 mm, Macherey-Nagel). The detection wavelength was 254 nm. Gradients of acetonitrile-
536 water with 0.1% TFA were used for elution at flow rates of 1 mL/min, 8 mL/min, and 14 mL/min on
537 the analytical, semi-preparative and preparative columns respectively. Melting points (mp) were
538 determined with Stuart Melting Point Apparatus SMP3 and are not corrected. Mass spectra were
539 recorded on a 4000Q TRAP LC/MS/MS/ System for AB Applied Biosystems MDS SCIEX. NMR
540 spectra were recorded on a Bruker AV300 spectrometer instrument operating at 300 MHz for proton
541 frequency using DMSO-*d*₆ solutions. Chemical shifts were quoted relative to the residual DMSO peak
542 (¹H: δ = 2.50 ppm, ¹³C: δ = 39.52 ppm). Coupling constants (J) are given in Hertz (Hz). Splitting patterns
543 are indicated as follows: singlet (s), doublet (d), triplet (t), quartet (q), multiple (m), broad (b). Purity of

544 each compound used for biological testing was $\geq 95\%$ unless otherwise noted. The purity check of known
 545 inhibitors purchased for comparison with our compounds are found in Supporting Information Figure
 546 S9.

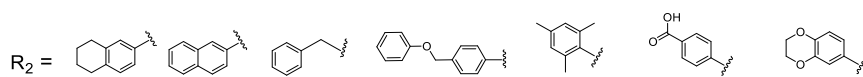
547

548 **Synthesis of compounds 8, 11 – 17**



550

$R_1 = CF_3, Br, Cl$



Feldfunktion geändert

551 **Scheme 3: Synthesis of compounds 8, 11 - 17**

552 To a solution of anthranilic acid substituted with the appropriate R_1 (1.32 mmol) and sodium carbonate
 553 (3.17 mmol) in water (2 mL) at 80 °C, the sulfonyl chloride (1.58 mmol) substituted with the appropriate
 554 R_2 was added over a period of 5 minutes. The stirring continued for 18 h at 80 °C. The reaction mixture
 555 was cooled to room temperature and acidified with 6 N HCl, and the resulting solid precipitate was
 556 filtered, washed with water and dried to give the crude product. The final product was obtained by
 557 preparative HPLC (Puranik 2008).

558

559 **2-(5,6,7,8-tetrahydronaphthalene-2-sulfonamido)-5-(trifluoromethyl) benzoic acid (8)**

560 (0.52 g, 74% yield) **¹H-NMR** (300 MHz, DMSO-d₆): $\delta = 11.77$ [s, 1H, COOH], 8.13 [s, 1H, NH],
 561 7.85 [d, $^3J_{6,4} = 2.1$ Hz, 1H, 6-H_{Ar}] 7.62 [d, $^4J_{1',3'} = 2.1$ Hz, 1H, 1'-H_{Ar}] 7.53 [dd, $^3J_{4,3} = 7.1$ Hz, $^4J_{4,6} =$
 562 2.1 Hz, 4-H_{Ar}] 7.36 [dd, $^3J_{3',4'} = 7.5$ Hz, $^4J_{3',1'} = 2.4$ Hz, 1H, 3'-H_{Ar}] 7.15 [d, $^3J_{4',3'} = 7.5$ Hz, 1H, 4'-H_{Ar}]
 563 , 6.90 [d, $^3J_{3,4} = 7.1$ Hz, 1H, 3-H_{Ar}] 2.73 (m, 4H, CH₂); 1.6 (m, 4H, CH₂); **¹³C-NMR** (75 MHz, DMSO-
 564 d₆): $\delta = 169.1$ (C, C_{Ar}-8), 152.7 (C, C_{Ar}-2), 143.8 (C, C_{Ar}-4a'), 138.7 (C, C_{Ar}-2'), 135.9 (C, C_{Ar}-8a'),

565 130.4(CH, C_{Ar}-4), 128.7 (CH, C_{Ar}-6), 127.5 (CH, C_{Ar}-1'), 124.0 (CH, C_{Ar}-4'), 121.6 (C, C-6), 118.2 (C,
566 C_{Ar}-5), 116.9 (C, C_{Ar}-3), 29.0 (CH₂, C-8'), 28.8 (CH₂, C-5'), 22.3 (CH₂, C-6'), 22.2 (CH₂, C-7'); mp:
567 177°C; MS (ESI) *m/z*: calcd. for C₁₈H₁₆F₃NO₄S, 399; found 400 [M+H]⁺.

568 **5-bromo-2-(naphthalene-2-sulfonamido) benzoic acid (11)**

569 (0.13 g, 67% yield) ¹H-NMR (300 MHz, DMSO-d₆): δ = 10.2 [s, 1H, COOH], 9.8 [s, 1H, NH] 8.59 [d,
570 ⁴J_{1',3'} = 1.4 Hz, 1 H, 1'-H_{Ar}], 8.17 [d, ³J_{8',7'} = 7.8 Hz, 1 H, 8'-H_{Ar}], 8.10 [d, ³J_{4',3'} = 8.8 Hz, 1 H, 4'-H_{Ar}],
571 8.02 [d, ³J_{5',6'} = 7.8 Hz, 1 H, 5'-H_{Ar}], 7.93 [d, ⁴J_{6,4} = 2.4 Hz, 1 H, 6-H_{Ar}], 7.77 [dd, ³J_{3',4'} = 8.8 Hz, ⁴J_{3',1'}
572 = 1.4Hz, 1 H, 3'-H_{Ar}], 7.72 – 7.65 [m, 3 H, 4-H_{Ar}, 6'-H_{Ar}, 7'-H_{Ar}], 7.51 [d, ³J_{3,4} = 8.9 Hz, 1 H, 3-H_{Ar}]. –
573 ¹³C-NMR (75 MHz, DMSO-d₆): δ = 168.2 (C, C-7), 138.8 (C, C_{Ar}-2), 136.8 (CH, C_{Ar}-4), 135.3 (C, C_{Ar}-
574 4a'), 134.4 (C, C_{Ar}-8a'), 133.4 (CH, C_{Ar}-6), 131.4 (CH, C_{Ar}-6'), 129.3 (CH, C_{Ar}-4'), 128.5 (CH, C_{Ar}-
575 8'), 127.8 (2xCH, C_{Ar}-5', C_{Ar}-7') 121.6 (CH, C_{Ar}-3'), 120.6 (CH, C_{Ar}-3), 119.0 (C, C_{Ar}-1), 114.9 (C, C_{Ar}-
576 5). Mp: 199°C; (ESI) *m/z*: calcd. for C₁₇H₁₁BrNO₄S⁻; 403.9560: found 403.9613 [M-H].

577 **5-bromo-2-(phenylmethylsulfonamido)benzoic acid (12)**

578 (0.07g, 42% yield) ¹H-NMR (300 MHz, DMSO-d₆): δ = 10.57 [s, 1 H, COOH], 8.05 [d, ⁴J_{6,4} = 2.4
579 Hz, 1 H, 6-H_{Ar}], 7.75 [dd, ³J_{4,3} = 8.9 Hz, ⁴J_{4,6} = 2.4Hz, 1 H, H-4_{Ar}], 7.49 [d, ³J_{3,4} = 8.9 Hz, 1 H, 3-H_{Ar}],
580 7.33 – 7.28 [m, 3 H, 3'-H_{Ar}, 5'-H_{Ar}], 7.23 – 7.20 [m, 2 H, 4'-H_{Ar}], 5.75 [s, 1 H, NH], 4.72 [s, 2 H, 1'-
581 H] ¹³C-NMR (75 MHz, DMSO-d₆): δ = 168.3 (C, C-7), 139.9 (C, C_{Ar}-2), 137(CH, C_{Ar}-4), 133.4 (CH,
582 C_{Ar}-6), 130.7 (CH, C_{Ar}-3'), 128.6 (C, C_{Ar}-2'), 128.4 (CH, C_{Ar}-5'), 128.3 (CH, C_{Ar}-4'), 119.5 (CH,
583 C_{Ar}-3), 117.5 (C, C_{Ar}-1), 113.9 (C, C_{Ar}-5), 57.4 (CH₂, C-1'). Mp: 216°C; (ESI) *m/z*: calcd. for
584 C₁₄H₁₁BrNO₄S⁻ 367.9860; found 367.9878 [M-H].

585 **5-bromo-2-(4-(phenoxy)methyl)phenylsulfonamido)benzoic acid (13)**

586 (0.6 g, 29% yield) ¹H-NMR (300 MHz, DMSO-d₆): δ = 7.97 [d, ⁴J_{6,4} = 2.4 Hz, 1 H, 6-H_{Ar}], 7.85 (d,
587 ³J_{2',3'} = 8.3 Hz, 2 H, 3'-H_{Ar}), 7.73 [dd, ³J_{4,3} = 8.9 Hz, ⁴J_{4,6} = 2.4Hz, 1 H, 4-H_{Ar}], 7.63 [d, ³J_{2',3'} = 8.3 Hz, 2
588 H, 2'-H_{Ar}], 7.47 [d, ³J_{3,4} = 8.9 Hz, 1 H, 3-H_{Ar}], 7.29 [dd, ³J_{3'',2''} = ³J_{3'',4''} = 7.3 Hz, 2 H, 3''-H_{Ar}], 7.00 – 6.92
589 [m, 3 H, 4''-H_{Ar}, 2''-H_{Ar}], 5.17 [s, H, 5'-H]. – ¹³C-NMR (75 MHz, DMSO-d₆): δ = 168.2 (C, C-7),
590 157.9 (C, C_{Ar}-1''), 143.2 (C, C_{Ar}-4'), 138.8 (C, C_{Ar}-2), 137.5 (C, C_{Ar}-1'), 136.9 (CH, C_{Ar}-4) 133.5 (CH,
591 C_{Ar}-6), 129.4(CH, C_{Ar}-3''), 128.1(CH, C_{Ar}-2'), 127.0 (CH, C_{Ar}-3'), 120.9 (CH, C_{Ar}-4''), 120.5 (CH, C_{Ar}-

592 3), 119.0 (C, C_{Ar}-1), 114.9 (CH, C_{Ar}-5), 114.7 (CH, C_{Ar}-2''), 68.0 (CH₂, C-5') Mp: 175°C; (ESI) m/z:
593 calcd for C₂₀H₁₅BrNO₅S- 459.9860 found 459.9878 [M-H]-.

594 **5-bromo-2-(2,4,6-trimethylphenylsulfoamido)benzoic acid (14)**

595 (0.6 g, 78% yield) ¹H-NMR (300 MHz, DMSO-d₆): δ = 11.77 [s, 1H, COOH], 9.98 [s, 1H, NH], 7.68
596 [d, ³J_{6,4} = 7.4 Hz, 1H, 6-H_{Ar}], 7.51 [dd, ³J_{4,3} = 7.1 Hz, ⁴J_{4,6} = 7.4 Hz, 1H 4-H_{Ar}], 7.17 [d, 2H, 4'-H_{Ar}, 6'-
597 H_{Ar}], 7.14 [d, ³J_{3,4} = 1H, 3-H_{Ar}], 2.56 [s, 6H, CH₃, 9'-H, 7'-H], 2.21 [s, 3H, CH₃, 8'-H]; -¹³C-NMR (300
598 MHz, DMSO-d₆): δ = 168.8 (C, C-7), 143.3 (C, C_{Ar}-2), 139.5 (C, C_{Ar}-2'), 139.0 and 139.0 (2xC, C_{Ar}-
599 3', C_{Ar}-1') 137.3 (CH, C_{Ar}-4), 134.0 (CH, C_{Ar}-6'), 133.0 (CH, C_{Ar}-6), 132.5 and 132.5 (2XCH, C_{Ar}-4',
600 C_{Ar}-6') 119.1 (CH, C_{Ar}-3), 117.9 (C, C_{Ar}-5), 114.3 (C, C_{Ar}-1), 22.5 and 22.5 (2 x CH₃, C-7', C-9') 20.7
601 (CH₃, C-8'); mp: 185; MS (ESI): m/z 399 [M+H]⁺.
602

603 **2-(4-acetylphenylsulfoamido)-5-(trifluoromethyl)benzoic acid (15)**

604 (0.4 g, 63% yield) ¹H-NMR (300 MHz, DMSO-d₆): δ = 12.28 [s, 1H, COOH]; 12.10 [s, 1H, NH], 8.11
605 [d, ⁴J_{6,4} = 2.5 Hz, 1H, 6-H_{Ar}], 8.08 [d, ³J_{3,2} = 7.5 Hz, 2H, 3'-H_{Ar}], 7.86 [dd, ⁴J_{4,6} = 2.5 Hz, ³J_{4,3} = 7.3 Hz,
606 1H, 4-H_{Ar}], 7.64 [d, ³J_{4,3} = 7.3 Hz, 1H, 3-H_{Ar}], 7.56 [dd ³J_{2,3} = 7.5 Hz, ⁴J_{2,6} = 2.3 Hz, 2H, 2'-H_{Ar}, 6'-
607 H_{Ar}] 7.22 [dd, ³J_{3,2} = 7.5 Hz, ⁴J_{3,5} = 2.1 Hz, 2H, 3'-H_{Ar}, 5'-H_{Ar}] 2.50 [s, 3H, CH₃, 8'-H]; -¹³C-NMR
608 (75 MHz, DMSO-d₆): δ = 197.9 (C, C-7'), 169.1 (C, C-8), 151.8 (C, C_{Ar}-2) 143.5 (C, C_{Ar}-1'), 142.5 (C,
609 C_{Ar}-4'), 140.6 (CH, C_{Ar}-4), 131.4 (CH, C_{Ar}-7), 129.6 (2XCH, C_{Ar}-3', C_{Ar}-5'), 128.6 (2XCH, C_{Ar}-2', C_{Ar}-
610 6'), 127.6 (C, C_{Ar}-6), 123.0 (C, C_{Ar}-5), 118.7 (CH, C_{Ar}-3), 27.3 (CH₃, C-8'); mp: 170°C; MS (ESI) m/z
611 : calcd. for C₁₆H₁₂F₃NO₅S. 387; found 388 [M+H]⁺.

612 **2-(2,3-dihydrobenzo[*b*][1,4]dioxine-6-sulfonamido)-5-(trifluoromethyl)benzoic acid (16)**

613 (0.4 g, 65% yield) ¹H-NMR (300 MHz, DMSO-d₆): δ = 11.48 [s, 1H, COOH], 8.13 [s, 1H, NH], 7.89
614 [d, ⁴J_{6,4} = 3.9 Hz, 1H, 6-H_{Ar}] 7.66 [dd, ³J_{4,3} = 7.2 Hz, ⁴J_{4,6} = 4.3 Hz, 1H, 4-H_{Ar}],
615 7.23 [d, ³J_{4,3} = 7.2 Hz 1H, 3-H_{Ar}], 7.11 [dd, ³J_{2,3} = 7.3 Hz, ⁴J_{2,8} = 3.2 Hz, 1H, 2'-H_{Ar}] 6.95 [d, ⁴J_{2,8} =
616 3.2 Hz, 1H, 8'-H_{Ar}] 4.23 – 4.31 [m, 4H, 5'-H, 6'-H]; -¹³C-NMR (75-MHz, DMSO-d₆): δ = 168.9 (C,
617 C-8), 148.3 (C, C-4'), 143.8 (C, C-2), 143.5 (C, C-7'), 131.3 (C, C-1'), 130.8 (CH, C-4), 128.6 (CH, C-
618 6), 125.7 (C, C-7), 122.1 (C, C-5), 120.9 (CH, C-2'), 118.3 (CH, C-3), 118.1 (CH, C-3'), 116.8 (CH, C-
619 8'), 64.7 (CH₂, C-5') 64.3 (CH₂, C-6'); mp: 178°C; MS (ESI) m/z: calcd. for C₁₆H₁₂F₃NO₆S. 403; found
620 404 [M+H]⁺.

621 **5-(trifluoromethyl)-2-(2,4,6-trimethylphenylsulfoamido)benzoic acid (17)**
622 (0.38 g, 62% yield) **¹H-NMR** (300 MHz, DMSO-*d*₆): δ = 12.28 [s, 1H, *COOH*], 11.60 [s, 1H, *NH*], 8.15
623 [d, ⁴J_{6,4} = 4.3 Hz, 1H, 6-*H_{Ar}*] 7.92 [dd, ³J_{4,3} = 7.9 Hz, ⁴J_{4,6} = 2.1 Hz, 1H, 4-*H_{Ar}*] 7.87 [d, ⁴J_{6',4} = 1.9 Hz, 2H,
624 4'-*H_{Ar}*, 6'-*H_{Ar}*], 7.48 [d, ³J_{3,4} = 7.9 Hz, 1H, 3-*H_{Ar}*], 2.60 [s, 6H, CH₃, 9'-H, 7'-H], 2.23 [s, 3H, CH₃,
625 8'-H]; - **¹³C-NMR** (75 MHz, DMSO-*d*₆): δ = 169.3 (C, C-7), 154.2 (C, C-2), 143.6 (C, C-2'), 139.1
626 and 139.1 (2xC, C-1', C-3') 132.9 (C, C-5'), 132.5 (CH, C-4), 131.5 and 131.5 (2xCH, C-4', C-6'),
627 130.1 (CH, C-6), 128.7 (C, C-8), 122.5 (C, C-5), 117.0 (CH, C-3), 109.0 (C, C-1), 22.4 and 22.4
628 (2xCH₃, C-7', C-9'), 20.8 (CH₃, C-8'); mp: 184°C; MS (ESI) *m/z*: calcd. for C₁₇H₁₆F₃NO₄S; 387: found
629 388 [M+H]⁺.

630

631 **18, 19, 20, and 21** were purchased from Enamine, Kiev, Ukraine as pure compounds (see also Table S6,
632 Supporting Information).

633

634 **Determination of ligand binding and binding constant by NMR**

635 50 μM of ¹⁵N-labeled protein samples were prepared in a 20 mM sodium phosphate buffer containing
636 50 mM sodium chloride, 0.02 % (w/v) NaN₃, at pH 7.4. Stock solutions of small molecules were
637 prepared in DMSO-*d*₆ at a concentration of 160 mM. A ¹H-¹⁵N HSQC spectrum of Dvl PDZ was
638 acquired at 300 K with 5% DMSO-*d*₆ in the absence of ligand as reference spectrum. Mixtures of 16
639 compounds were added to ¹⁵N-labeled Dvl PDZ at 8-fold molar excess each. The final concentration of
640 DMSO-*d*₆ in the protein-ligand solutions was 5%. Spectra were acquired with 8 scans and 256 points
641 in the indirect dimension.

642 Binding was deduced if the resonance position of a cross-peak was significantly shifted compared to the
643 reference spectrum. The active compound was obtained through successive deconvolution. Experiments
644 were recorded on a Bruker DRX600 spectrometer equipped with a triple-resonance cryoprobe. The
645 preparation of samples was done automatically by a Tecan Genesis RSP 150 pipetting robot. Spectra
646 were analysed using the programs TOPSPIN and SPARKY.

647 Chemical shift perturbations were obtained by comparing the ^1H - ^{15}N backbone resonances of protein
648 alone to those of protein-ligand complex. The mean shift difference ($\Delta\delta$ in ppm) was calculated using
649 the equation 1 (Garrett 1997, Bertini 2011).

$$650 \quad \Delta\delta = \sqrt{\frac{[\Delta\delta_H]^2 + [\Delta\delta_N/5]^2}{2}} \quad (\text{Eq. 1})$$

651 Here $\Delta\delta_N$ and $\Delta\delta_H$ are the amide nitrogen and amide proton chemical shift differences between the free
652 and the bound states of the protein. In order to estimate binding constants, titration experiments
653 monitored by NMR were done. A series of ^1H - ^{15}N HSQC were recorded as a function of ligand
654 concentration. Residues showing a continuous chemical shift change and for which the intensity
655 remained strong were classified as being in fast exchange. The dissociation binding constant was
656 estimated by fitting the observed chemical shift change to equation 2 (Shuker 1996, Hajduk 1997).

$$657 \quad \frac{\Delta\delta}{\Delta\delta_{max}} = \frac{([L_T] + [P_T] + K_D) - \sqrt{([L_T] + [P_T] + K_D)^2 - 4[L_T] \cdot [P_T]}}{2[P_T]} \quad (\text{Eq. 2})$$

659
660 $\Delta\delta$ is the observed protein amide chemical shift change at a given compound concentration and $\Delta\delta_{max}$
661 the maximum chemical shift change at saturation. $[L_T]$ the total concentration of the compound, and $[P_T]$
662 the total concentration of the protein. K_D is the equilibrium dissociation constant. The K_D values are
663 reported as means \pm standard deviations of at least six residues influenced upon binding of the ligand.

664

665 **Determination of binding constant by Isothermal Titration Calorimetry (ITC)**

666 Isothermal Titration Calorimetry (ITC) experiments were performed using a VP-ITC system
667 (MicroCal). Protein in 20 mM Hepes buffer, 50 mM NaCl, pH 7.4, was centrifuged and degassed before
668 the experiment. A 200 μM ligand solution containing 2% DMSO was injected 30 times in 10 μL aliquots
669 at 120 s intervals with a stirring speed of 1000 rpm into a 1.4 mL sample cell containing the Dvl PDZ
670 domain at a concentration of 20 μM at 25 $^\circ\text{C}$. Control experiment was initially determined by titrating
671 ligand into buffer at same conditions. Titration of ligand into buffer yielded negligible heats.

672 Thermodynamic properties and binding constants were determined by fitting the data with a nonlinear
673 least-squares routine using a single-site binding model with Origin for ITC v.7.2 (Microcal).

674

675 **Protein expression**

676 PDZ domains of human AF6 (P55196-2, residues 985–1086) and murine α 1-syntrophin (Q61234,
677 residues 81–164) were cloned into pGEX-6P-2 (Amersham Biosciences, Freiburg, Germany) and
678 pGAT2 (European Molecular Biology Laboratory, Heidelberg, Germany), respectively. Proteins were
679 expressed in *E. coli* BL21 (DE3) cells and purified as previously described (Boisguerin 2004). For the
680 cloning of the Dvl-1 PDZ domain (O14640, residues 245–338), IMAGp958J151157Q (ImaGenes) was
681 used as template. V250 is exchanged to isoleucine as in human Dvl-3 or murine Dvl-1. The C-terminal
682 C338 of the domain was exchanged by serine. Via cloning in pET46EK/LIC, a coding sequence for a
683 TEV (Tobacco Etch Virus) protease cleavage site was introduced. The resulting plasmid pDVL1 was
684 transformed in *E. coli* BL21 (DE3). Expression on two-fold M9 minimal medium with 0.5 g/L ^{15}N
685 NH_4Cl as sole nitrogen source in shaking culture was done at 25 °C overnight with 1 mM IPTG. A yield
686 of 25 mg of pure Dvl-1 was obtained from 1 L culture after IMAC, TEV protease cleavage, a second
687 IMAC, and gel filtration (Superdex 75). The protein domain Dvl-1_245–338 was supplied for NMR in
688 20 mM phosphate buffer, pH 7.4, 50 mM NaCl.

689 The production of Dvl-3 (Q92997 residues 243-336), mShank3 (Q4ACU6, residues 637-744) PDZ
690 domains and the 3 PDZ domains of PSD95 was described by Saupe et al (Saupe 2011).

691

692 **Crystallization and X-ray diffraction**

693 The His-tagged cleaved human Dvl-3 PDZ domain was concentrated to 12-20 mg/mL in the presence
694 of a 5-fold molar excess of compound **3**, **5**, **6**, **7**, **11** and **12**. Crystals of all complexes were grown at
695 room temperature by the sitting drop vapour-diffusion method. 200 nL Dvl-3/compound solution was
696 mixed with an equal volume of reservoir solution using the Gryphon (Formulatrix) pipetting robot.
697 Crystals of all complexes were grown to their final size within 4 to 14 days. The Dvl-3 PDZ domain
698 crystallized in complex with compound **3** and **7** in crystallization condition 30% PEG 8000, 0.2 M
699 ammonium sulphate, 0.1 M MES pH 6.5; with compound **5** in 30% PEG 8000, 0.1 M MES pH 5.5; with

700 compound **6** in 1.2 M ammonium sulphate, 0.1 M citric acid pH 5.0; with compound **12** in 32% PEG
701 8000, 0.2 M ammonium sulphate, 0.1 M Na-cacodylate pH 6.0; with compound **11** in 1 M ammonium
702 sulphate, 1% PEG 3350, 0.1 M Bis-Tris pH 5.5; with compound **12** in 1.26 M sodium phosphate, 0.14
703 M potassium phosphate and with compound **18** in 1.5 M ammonium sulphate, 12% glycerol, 0.1 M Tris-
704 HCl pH 8.5. The crystals were cryoprotected if necessary, for data collection by soaking for few seconds
705 in precipitant solution containing 20% (v/v) glycerol and subsequently frozen in liquid nitrogen.
706 Diffraction data were collected at 100 K at beamline BL14.1 at the synchrotron-radiation source BESSY,
707 Helmholtz-Zentrum Berlin and processed with XDS.

708

709 **Structure determination and refinement**

710 Phases for the Dvl-3 PDZ domain in complex with compound **3** were obtained by molecular replacement
711 with PHASER (McCoy 2007) using the *Xenopus laevis* Dishevelled PDZ domain structure (PDB code
712 2F0A) as a starting model. The reasonable crystal packing and electron density allowed further model
713 and compound building using the program COOT (Emsley 2004) with iterative refinement with
714 REFMAC (Murshudov 1997). All further complex structures were obtained in the same way but using
715 the final refined compound free Dvl-3-PDZ structure as model for molecular replacement. The
716 Ramachandran statistics were analysed by Molprobit (Chen 2010) for all complexes and all
717 crystallographic statistics are given in Supporting Information Tables S2 and S3. Figures were prepared
718 with PyMol. Atomic coordinates and structure factor amplitudes for DVL-3 PDZ domain in complex
719 with compound **3**, **5**, **6**, **7**, **11**, **12**, **18** were deposited in the Protein Data Bank with accession codes
720 6ZBQ, 6ZBZ, 6ZC3, 6ZC4, 6ZC6, 6ZC7 and 6ZC8, respectively.

721

722 **MTT assay**

723 HEK293 cells were plated on a 96-well plate and treated with different concentrations of Dvl inhibitors.
724 After 24 h treatment, 20 μ l of MTT solution (5 mg/mL) was added into each well. After 2 h incubation,
725 cell culture medium was replaced with 50 μ L DMSO, and the signal of the purple formazan, produced
726 by living cells, was measured by a plate reader.

727

728 **TOP-GFP reporter assay**

729 The lentivirus particle (CCS-018L, SABiosciences) encoding GFP under the control of a basal promoter
730 element (TATA box) joined to tandem repeats of a consensus TCF/LEF binding site was transfected
731 into HEK293 cells. Stable cells were selected by puromycin (2 µg/mL) treatment. Wnt signalling
732 activity indicated by GFP intensity was measured by flow cytometry after 24 h incubation with
733 recombinant mouse Wnt3a (100 ng/mL) or GSK3 inhibitor CHIR99021 (3 µM) in the presence of Dvl
734 inhibitors.

735

736 **Luciferase reporter assays**

737 Plasmids encoding a firefly luciferase reporter gene under the control of different responsive elements
738 were transfected into HeLa cells with a pRL-SV40 normalization reporter plasmid using the
739 Lipofectamine 2000 (Invitrogen). After desired treatment, cells were harvested in the passive lysis buffer
740 (Promega), and 15 µL cell lysate were transferred to 96-well LumiNunc plates (Thermo Scientific).
741 Firefly luciferase and Renilla luciferase were detected with the D-luciferin buffer (75 mM Hepes, 4 mM
742 MgSO₄, 20 mM DTT, 100 µM EDTA, 0.5 mM ATP, 135 µM Coenzyme A and 100 µM D-Luciferin
743 sodium salt, pH 8.0) and the coelenterazine buffer (15 mM Na₄PPi, 7.5 mM NaAc, 10 mM CDTA, 400
744 mM Na₂SO₄, 25 µM APMBT and 1.1 µM coelenterazine, pH 5.0) respectively using the CentroXS
745 LB960 lumiometer (Berthold Technologies).

746

747 **Immunoblotting**

748 To assess the β-catenin accumulation in HeLa cells, cells were treated with Wnt3a in the presence of Dvl
749 inhibitors for 24 h and lysed in RIPA buffer (50 mM Tris, pH 8.0, 1% NP-40, 0.5% deoxycholate, 0.1%
750 SDS, 150 mM NaCl). Equal amounts of protein were loaded on a SDS-PAGE. Separated proteins were
751 blotted onto PVDF membranes for immunoblot analysis using anti-β-catenin antibody (610154, BD).
752 HRP-conjugated anti-mouse antibody (715-035-150, Jackson ImmunoResearch laboratories) was used
753 for secondary detection with Western lightning chemiluminescence reagent plus (PerkinElmer) and
754 Vilber Lourmat imaging system SL-3.

755

756 **qRT-PCR analysis**

757 To measure the Wnt target accumulation at mRNA level, HeLa cells were treated with Wnt3a in the
758 presence of Dvl inhibitors for 24 h. mRNA was extracted according to the standard TRIzol® protocol
759 (Invitrogen) and reverse-transcribed using random primers (Invitrogen) and M-MLV reverse
760 transcriptase (Promega). The qRT-PCR was performed in iQ5 Multicolor Real-Time PCR Detection
761 System (Bio-Rad) using SYBR® Green (Thermo Scientific) and gene-specific primer pairs of Bmp2,
762 Axin2, Lef1 and β -actin (endogenous control).

763

764 **Migration assay**

765 Cell motility was assessed using 24-well transwell (pore diameter: 8 μ m, Corning). SW480WL cells
766 were seeded in the upper chamber in serum free DMEM with 0.1% BSA; 20% serum was supplemented
767 to medium in the lower chamber. After incubation with Wnt3a in the presence of Dvl inhibitors for 24
768 h, nonmigrant cells were scraped off using a cotton swab; the migrated cells on the filters were stained
769 with DAPI, photographed and counted.

770

771 **Colon sphere culture**

772 SW480WL cells were trypsinised into single cells, seeded on 24-well cell culture plates precoated with
773 250 μ l polyhema (12 mg/mL in 95% ethanol, Sigma) per well, and incubated with Wnt3a in the presence
774 of Dvl inhibitors in the sphere culture medium (F12 : DMEM 1 : 1, 1X B-27 supplement, 20 ng/mL
775 EGF, 20 ng/mL FGF, 0.5% methylcellulose) for 10 days. Numbers of spheres were then counted under
776 the microscope.

777

778 **Notes**

779 The authors declare no competing financial interest.

780

781 **ACKNOWLEDGEMENTS**

782 This research was supported by the Deutsche Forschungsgemeinschaft (DFG) Research Group 806 and
783 the EU-project iNext (Infrastructure for NMR, EM and X-rays for Translational Research, GA 653706).

784 We thank M. Leidert and S. Radetzki for protein preparation, and B. Schlegel for NMR assistance. We
785 also thank E. Specker for compound analysis.

786 **ABBREVIATIONS USED**

787 NMR, nuclear magnetic resonance; HSQC, Heteronuclear Single Quantum Correlation;
788 AU, asymmetric unit; SAR, derive structure activity relationships; vdW, van der Waals;
789 ITC, Isothermal titration calorimetry; PDZ, PSD95/Disc large/Zonula occludens 1);
790 Dvl, Dishevelled; PPI, protein-protein interactions; PDB, Protein Data Bank;
791 CSP, chemical shift perturbation; GFP, green fluorescent protein; DMSO, dimethyl sulfoxide;
792 PEG, polyethylene glycol; RNA, ribonucleic acid; mRNA, messenger RNA;
793 qRT-PCR, quantitative real-time polymerase chain reaction; DMEM Dulbecco's modified Eagle's
794 medium ; BSA, bovine serum albumin;

795

796 **ASSOCIATED CONTENT**

797

798 **Accession Codes**

799 Atomic coordinates and structure factor amplitudes for DVL3 PDZ domain in complex with compound
800 **3, 5, 6, 7, 11, 12, 18** were deposited in the Protein Data Bank with accession codes 6ZBQ, 6ZBZ, 6ZC3,
801 6ZC4, 6ZC6, 6ZC7 and 6ZC8, respectively. Authors will release the atomic coordinates and
802 experimental data upon article publication.

803

804 **Supporting information**

805 **1.** Structure-based alignment of the amino acid sequences of Dvl-1,2,3 PDZ ; PSD95-PDZ-1,2,3 ; Af-
806 6 and Syn PDZ domains. (S.2)

807 **2.** ¹H-¹⁵N HSQC spectra of Dvl-3 PDZ domain alone and in the presence of varying concentrations of
808 compound 3. (S.3)

809 **3.** Detailed views of diverse compounds bound to the Dvl-3 PDZ domain. (S.4)

810 **4.** Cell viability assays of compounds 3, 7,8, 9, 10, (A) and 18, 20, 21 (B). (S.5)

811 **5.** ITC binding assays of compound 18 with Dvl-3 PDZ (A) and with Dvl-1 PDZ (B). (S.5)

812 6. Structures of selected compounds used for comparison to our compounds. (S.6)

813 7. ITC data of selected compounds used for comparison to our compounds. (S.7)

814 8. [NMR binding assay with compound 322338/3289-8625. \(S.8\)](#)

815 9. Purity check of compounds. (S.9)

816 – Purity check of NPL-1011 compound. (S.9)

817 – Purity check of Sulindac compound. (S.10)

818 – Purity check of CalBioChem-322338 compound. (S.11)

819 – Purity check of NSC668036 compound. (S.12)

820 – LCMS of intermediate compound 8. (S.13)

821 – LCMS of intermediate compound 14. (S.13)

822 10. Chemical shift perturbation values of Dvl-3 PDZ and Dvl-1 PDZ for compounds (3-21). (S.14)

823 11. Data collection and refinement statistics of compounds 3, 5, 6, 7. (S.15)

824 12. Data collection and refinement statistics of compounds 11, 12, 18. (S.16)

825 13. Selectivity of ligands derived from chemical shift perturbation of compounds tested at other PDZ

826 domains. (S.17)

827 14. Details of Multifilter routines. (S.17)

828 15. Smiles codes and Compounds ID. (S.18)

829 16. NMR characterization of synthesized compounds (8, 11, 13, 14, 15, 16, 17). (S.21)

830

831 **References**

832 Behrens, J., von Kries, J. P., Kühl, M., Bruhn, L., Wedlich, D., Grosschedl, R. and Birchmeier, W.:
833 Functional interaction of beta-catenin with the transcription factor LEF-1. *Nature*, 382, 638-642,
834 DOI: 10.1038/382638a0, 1996.

835 Bertini, I., Chevanace, S., Del Conte, R., Lalli, D. and Turano, P.: The anti-apoptotic Bcl-x(L) protein,
836 a new piece in the puzzle of cytochrome c interactome. *PLoS One*, 6:e18329, DOI:
837 10.1371/journal.pone.0018329, 2001.

838 Berman, H. M., Westbrook, J., Feng, Z., Gilliland, G., Bhat, T. N., Weissig, H., Shindyalov, I. N. and
839 Bourne, P.E.: The protein data bank, *Nucleic. Acids Res.*, 28, 235 – 242, DOI: 10.1093/nar/28.1.235,
840 2000.

841 Boisguerin, P., Leben, R., Ay, B., Radziwill, G., Moelling, K., Dong, L. and Volkmer-Engert, R.: An
842 improved method for the synthesis of cellulose membrane-bound peptides with free C termini is
843 useful for PDZ domain binding studies. *Chem. Biol.*, 11, 449 – 459, DOI:
844 10.1016/j.chembiol.2004.03.010, 2004.

845 Bui, T. D., Beier, D. R., Jonssen, M., Smith, K., Dorrington, S. M., Kaklamanis, L., Kearney, L.,
846 Regan, R., Sussman, D. J. and Harris, A. L.: cDNA cloning of a human dishevelled DVL-3 gene,

hat gelöscht: Definition of PDZ binding site. (S.8)

848 mapping to 3q27, and expression in human breast and colon carcinomas. *Biochem. Biophys. Res.*
849 *Commun.*, 239, 510 – 516, DOI: 10.1006/bbrc.1997.7500, 1997.

850 Chandanamali, P., Antonio, M. F., Robert, C., Patrick, R. and Naoaki, F.: Sequence and subtype
851 specificity in the high-affinity interaction between human frizzled and dishevelled proteins, *Protein*
852 *Sci.*, 18, 994 – 1002, DOI: 10.1002/pro.109, 2009.

853 Chen V. B., Arendall, W. B. 3rd, Headd, J. J. and Keedy, D. A., Immormino, R. M., Karpral, G. J.,
854 Murray, L. W., Richardson, J. S., Richardson, D. C.: MolProbity: all-atom structure validation for
855 macromolecular crystallography. *Acta Cryst.*, 66, 12 - 21, DOI: 10.1107/S0907444909042073, 2010.

856 Choi, J., Ma, S.; Kim, H.-Y., Yun, J.-H., Heo, J.-N., Lee, W., Choi, K.-Y. and No, K.: Identification of
857 small-molecule compounds targeting the dishevelled PDZ domain by virtual screening and binding
858 studies. *Bioorg. Med. Chem.*, 24, 3259–3266. [Doi: 10.1016/j.bmc.2016.03.026](#), 2016.

859 Christensen, N. R., De Luca, M., Lever, M. B., Richner, M., Hansen, A. B., Noes-Holt, G., Jensen, K.
860 L., Rathje, M., Jensen, D. B., Erlendsson, S., Bartling, C. R., Ammendrup-Johnsen, I., Pedersen, S.
861 E., Schönauer, M., Nissen, K. B., Midtgaard, S. R., Teilum, K., Arleth, L., Sørensen, A. T., Bach, A.,
862 Strømgaard, K., Meehan, C. F., Vaegter, C. B., Gether, U. and Madsen, K. L.: A high-affinity,
863 bivalent PDZ domain inhibitor complexes PICK1 to alleviate neuropathic pain. *EMBO Mol. Med.*,
864 12 :e11248, DOI: 10.15252/emmm.201911248, 2020.

865 [Christensen, N. R., Calyseva, J., Fernandes, E. F. A., et al.: PDZ Domains as Drug Targets. *Adv.*
866 *Ther.*, 2\(7\), 1800143, \[Doi:10.1002/adtp.201800143\]\(#\), 2019.](#)

867 Chuprina, A., Lukin, O., Demoiseaux, R., Buzko, A. and Shivanyuk, A.: Drug- and lead-likeness,
868 target class, and molecular diversity analysis of 7.9 million commercially available organic
869 compounds provided by 29 suppliers. *J. Chem. Inf. Model.*, 50, 470 - 499. Doi: 10.1021/ci900464s,
870 2010.

871 Doyle, D. A., Lee, A., Lewis, J., Kim, E., Sheng, M. and MacKinnon, R.: Crystal structures of a
872 complexed and peptide-free membrane protein-binding domain: Molecular basis of peptide
873 recognition by PDZ. *Cell*, 85, 1067-1076, DOI: 10.1016/s0092-8674(00)81307-0, 1996.

874 Emsley, P. and Cowtan, K.: Coot: model-building tools for molecular graphics. *Acta Cryst.*, 60, 2126
875 – 2132 , DOI: 10.1107/S0907444904019158, 2004.

876 Fan, X., Quyang, N., Teng, H. and Yao, H.: Isolation and characterization of spheroid cells from the
877 HT29 colon cancer cell line. *Int. J. Colorect. Dis.*, 26, 1279 - 1285, DOI: 10.1007/s00384-011-1248-
878 y, 2011.

879 Fang, L., Von Kries, J. P. and Birchmeier, W.: Identification of small-molecule antagonists of the
880 TCF/ β -catenin protein complex, in 30 years of Wnt signalling. *EMBO Conference: Egmond aan Zee*,
881 Netherlands. p. 101, 2012.

882 Fanning, A. S. and Anderson, J. M.: Protein-protein interactions: PDZ domain networks. *Curr. Biol.*,
883 6, 1385 – 1388, DOI: 10.1016/s0960-9822(96)00737-3, 1996.

884 Fritzmann, J., Morkel, M., Besser, D., Budczies, J., Kosel, F., Brembeck, F. H., Stein, U., Fichtner, I.,
885 Schlag, P. M. and Birchmeier, W.: A colorectal cancer expression profile that includes transforming
886 growth factor beta inhibitor BAMB1 predicts metastatic potential. *Gastroenterology*, 137, 165 - 175,
887 DOI: 10.1053/j.gastro.2009.03.041, 2009.

888 Fujii, N., You, L., Xu, Z., Uematsu, K., Shan, J., He, B., Mikami, I., Edmondson, L.R., Neale, G.,
889 Zheng, J., Guy, R. K. and Jablons, D. M.: An antagonist of dishevelled protein-protein interaction
890 suppresses β -catenin-dependent tumor cell growth. *Cancer Res.*, 67, 573 - 579, DOI: 10.1158/0008-
891 5472.CAN-06-2726, 2007.

892 Garrett, D. S., Seok Y. J., Peterkofsky A. and Gronenborn, A. M.: Identification by NMR of the
893 binding surface for the histidine-containing phosphocarrier protein HPr on the N-terminal domain of
894 enzyme I of the Escherichia coli phosphotransferase system. *Biochem.*, 36, 4393 – 4398, DOI:
895 10.1021/bi970221q, 1997.

896 Goddard, T. D. and Kneller, D. G.: SPARKY 3, University of California, San Francisco, 2003.

897 Grandy, D., Shan, J., Zhang, X., Rao, S., Akunuru, S., Li, H., Zhang, Y., Alpatov, I., Zhang, X., Lang,
898 R., Shi, De-Li. and Zheng, J.: Discovery and characterization of a small molecule inhibitor of the
899 PDZ domain of dishevelled. *J. Biol. Chem.*, 284, 16256–16263. DOI: 10.1074/jbc.M109.00 9647,
900 2009.

901 Hajduk, P. J., Sheppard, G., Nettesheim, D. G., Olejniczak, E. T., Shuker, S. B., Meadows, R. P.,
902 Steinman, D. H., Carrera, G. M. Jr., Marcotte, P. A., Severin, J., Walter, K., Smith, H., Gubbins, E.,
903 Simmer, R., Holzman, T. F., Morgan, D. W., Davidsen, S. K., Summers, J. B. and Fesik, S. W.:

hat gelöscht: DOI

hat formatiert: Englisch (USA)

hat formatiert: Englisch (USA)

Feldfunktion geändert

Feldfunktion geändert

Feldfunktion geändert

Feldfunktion geändert

Feldfunktion geändert

Feldfunktion geändert

905 Discovery of Potent Nonpeptide Inhibitors of Stromelysin Using SAR by NMR. *J. Am. Chem. Soc.*,
906 119, 5818 – 5827, DOI: 10.1021/ja9702778, 1997.

907 Hammond, M.C., Harris, B. Z., Lim, W. A., Bartlett, P. A.: β Strand Peptidomimetics as Potent PDZ
908 Domain Ligands. *Chem. Biol.*, 13(12), 1247-1251, DOI: 10.1016/j.chembiol.2006.11.010, 2006.

909 Harris, B. Z., Lau, F. W., Fujii, N., Guy, R. K. and Lim, W. A.: Role of electrostatic interactions in
910 PDZ domain ligand recognition. *Biochem.*, 42, 2797-2805, DOI: 10.1021/bi027061p, 2003.

911 Haugaard-Kedström, L. M., Clemmensen, L. S., Sereikaite, V., Jin, Z., Fernandes, E. F. A., Wind, B.,
912 Abalde-Gil, F., et al.: A High-Affinity Peptide Ligand Targeting Syntenin Inhibits Glioblastoma. *J.*
913 *Med. Chem.* 64(3), 1423-1434, DOI: 10.1021/acs.jmedchem.0c00382, 2021.

914 Hegedüs, Z., Hóbor, F., Shoemark, D. K., Celis, S., Lian, L.-Y., Trinh, Ch. H., Sessions, R. B.,
915 Edwards, T. A., Wilson, A. J.: Identification of β -strand mediated protein–protein interaction
916 inhibitors using ligand-directed fragment ligation. *Chem. Sci.*, 12, 2286, DOI: 10.1039/d0sc05694d,
917 2021.

918 Hillier, B. J., Christopherson, K. S., Prehoda, K. E., Bredt, D. S. and Lim, W. A.: Unexpected modes
919 of PDZ domain scaffolding revealed by structure of nNOS–synaptrophin complex. *Science*, 284, 812–
920 815, 1999.

921 Holland, J. D., Klaus, A., Garratt, A. N. and Birchmeier, W.: Wnt signaling in stem and cancer stem
922 cells. *Curr. Opin. Cell Biol.*, 25, 254-264, DOI: 10.1016/j.ceb.2013.01.004, 2013.

923 Hori, K., Ajioky, K., Goda, N., Shindo, A., Tagagishi, M., Tenno, T. and Hiroaki, H.: Discovery of
924 Potent Dishevelled/Dvl Inhibitors Using Virtual Screening Optimized With NMR-Based Docking
925 Performance Index. *Front. Pharmacol.*, 9, 983, DOI: 10.3389/fphar.2018.00983, 2018.

926 Jain, A.K. and Dubes, R.C. Upper Saddle River, NJ: Prentice Hall, Algorithms for clustering data.
927 320p, 1988.

928 Jho, E. H., Zhang, T., Domon, C., Joo, C.-K., Freund, J.-N. and Costantini, F.: Wnt/beta-catenin/Tcf
929 signaling induces the transcription of Axin2, a negative regulator of the signaling pathway. *Mol.*
930 *Cell. Biol.*, 22, 1172 - 1183, DOI: 10.1128/mcb.22.4.1172-1183.2002, 2002.

931 Kanwar, S. S., Yu, Y., Nautyal, J., Patel, B. B. and Majumdar, A. P. N.: The Wnt/beta-catenin
932 pathway regulates growth and maintenance of colonospheres. *Mol. Cancer.*, 9, 212, DOI:
933 10.1186/1476-4598-9-212, 2010.

934 Kim, H. Y., Choi, S., Yoon, J. H., Lim, H. J., Lee, H., Choi, J., Ro, E. J., Heo, J. N., Lee, W., No, K.
935 T. and Choi, K. Y.: Small molecule inhibitors of the Dishevelled-CXXC5 interaction are new drug
936 candidates for bone anabolic osteoporosis therapy. *EMBO Mol. Med.*, 8, 375-387, DOI:
937 10.15252/emmm.201505714, 2016.

938 Klaus, A. and Birchmeier, W.: Wnt signalling and its impact on development and cancer. *Nat. Rev.*
939 *Cancer*, 8, 387-398, DOI: 10.1038/nrc2389, 2008.

940 Kurakin, A., Swistowski, A., Wu, S. C. and Bredesen, D. E.: The PDZ domain as a complex adaptive
941 system. *PLoS One*, 2(9), e953, DOI: 10.1371/journal.pone.0000953, 2007.

942 Lee, I., Choi, S., Yun, J. H., Seo, S. H., Choi, S., Choi, K. Y. and Lee, W.: Crystal structure of the
943 PDZ domain of mouse Dishevelled 1 and its interaction with CXXC5. *Biochem. Biophys. Res.*
944 *Commun.*, 485, 584-590, DOI: 10.1016/j.bbrc.2016.12.023, 2017.

945 Lee, H. J., Wang, N. X., Shi, D. L. and Zheng, J. J.: Sulindac inhibits canonical Wnt signaling by
946 blocking the PDZ domain of the protein dishevelled. *Angew. Chem. Int. Ed. Engl.*, 48, 6448 - 6452,
947 DOI: 10.1002/anie.200902981, 2009.

948 Lee, H. J., Wang, X. N., Shao, Y. and Zhenz, J. J.: Identification of tripeptides recognized by the PDZ
949 domain of Dishevelled. *Bioorg. Med. Chem.*, 17, 1701 – 1708, 2009.

950 Lewis, A., Segditsas, S., Deheragoda, M., Pollard, P., Jeffery, R., Nye, E., Lockstone, H., Davis, H.,
951 Clark, S., Stamp, G., Poulson, R., Wright, N. and Tomlinson, I.: Severe polyposis in Apc(1322T)
952 mice is associated with submaximal Wnt signalling and increased expression of the stem cell marker
953 Lgr5. *Gut.*, 59, 1680 - 1686, DOI: 10.1136/gut.2009.193680, 2010.

954 Lipinski, C. A.: Drug-like properties and the causes of poor solubility and poor permeability. *J.*
955 *Pharmacol. Toxicol. Meth.*, 44, 235 – 249. DOI : 10.1016/s1056-8719(00)00107-6, 2000.

956 Lipinski, C. A., Lombardo, F., Dominy, B. W. and Feeney, P. J.: Experimental and computational
957 approaches to estimate solubility and permeability in drug discovery and development settings. *Adv.*
958 *Drug Deliv. Rev.*, 23, 3 – 25. DOI : 10.1016/S0169-409X(96)00423-1, 1997.

hat formatiert: Englisch (USA)

hat formatiert: Schriftart: 11 Pt., Nicht Kursiv

hat formatiert: Schriftart: 11 Pt.

hat formatiert: Schriftart: 11 Pt.

hat formatiert: Schriftart: 11 Pt.

hat formatiert: Schriftart: 11 Pt.

hat formatiert: Deutsch

hat formatiert: Deutsch

hat formatiert: Englisch (USA)

hat verschoben (Einfügung) [1]

hat gelöscht: ¶

960 Lv, P. C., Zhu, H. L., Li, H. Q., Sun, J. and Zho, Y.: Synthesis and biological evaluation of pyrazole
 961 derivatives containing thiourea skeleton as anticancer. *Bioorg. Med. Chem.*, 18, 4606 - 4614, DOI:
 962 10.1016/j.bmc.2010.05.034, 2010.

963 [Madrzak, J., Fiedler, M., Johnson, Ch. et al.: Ubiquitination of the Dishevelled DIX domain blocks its
 964 head-to-tail polymerization. *Nat. Commun.* 6, 6718, DOI: 10.1038/ncomms7718, 2015.](#)

965 Malanchi, I., Peinado, H., Kassen, D., Husenet, T., Metzger, D., Chambon, P., Huber, M., Hohl, D.,
 966 Cano, A., Birchmeier, W. and Huelsken, J.: Cutaneous cancer stem cell maintenance is dependent on
 967 beta-catenin signalling. *Nature.*, 452, 650 - 653, DOI: 10.1038/nature06835, 2008.

968 Mathvink, R. J., Barritta, A. M., Candelore, M. R., Cascieri, M. A., Deng, L., Tota, L., Strader, C. D.,
 969 Wyvratt, M. J., Fosher, M. H. and Weber, A. E.: Potent, elective human beta3 adrenergic receptor
 970 agonists containing a substituted indoline-5-sulfonamide pharmacophore. *Bioorg. Med. Chem. Lett.*,
 971 9, 1869 - 1874, DOI: 10.1016/s0960-894x(99)00277-2, 1999.

972 McCoy, A. J., Grosse-Kunstleve, R. W., Adams, P. D., Winn, M. D., Storoni, L. C. and Read, R. J.:
 973 Phaser crystallographic software. *J. Appl. Cryst.*, 40(Pt4), 658 - 674, DOI:
 974 10.1107/S0021889807021206, 2007.

975 McMartin, C. and Bohacek, R. S.: Powerful, rapid computer algorithms for structure-based drug
 976 design. *J. Computer-Aided Mol. Des.*, 11, 333 - 344, DOI: 10.1023/a:1007907728892, 1997.

977 Mizutani, K., Miyamoto, S., Nagahata, T., Konishi, N., Emi, M. and Onda, M.: Upregulation and
 978 overexpression of DVL1, the human counterpart of the Drosophila Dishevelled gene, in prostate
 979 cancer. *Tumori*, 91, 546 - 551, 2005.

980 Molenaar, M., van de Wetering, M., Oosterweeg, M., Peterson-Maduro, J., Godsave, S., Korinek,
 981 V., Roose, J., Destree, O. and Clevers, H.: XTcf-3 transcription factor mediates beta-catenin-induced
 982 axis formation in *Xenopus* embryos. *Cell.*, 86, 391 - 399, DOI: 10.1016/s0092-8674(00)80112-9,
 983 1996.

984 Mosmann, T.: Rapid colorimetric assay for cellular growth and survival: application to proliferation
 985 and cytotoxicity assays. *J. Immunol. Methods.*, 65, 55 - 63, DOI: 10.1016/0022-1759(83)90303-4,
 986 1983.

987 Murshudov, G. N., Vagin, A. A. and Dodson, E. J.: Refinement of macromolecular structures by the
 988 maximum-likelihood method. *Acta Cryst.*, 53, 240 - 255, DOI: 10.1107/S0907444996012255, 1997.

989 O'Brien, P. M., Ortwin, D. F., Pavlovsky, A. G., Picard, J. A., Sliskovic, D. R., Roth, B. D., Dyer, R.
 990 D., Johnson, L. L., Man, C. F. and Hallak, H.: Structure-activity relationships and pharmacokinetic
 991 analysis for a series of potent, systemically available biphenylsulfonamide matrix metalloproteinase
 992 inhibitors. *J. Med. Chem.*, 43, 156 - 166, DOI: 10.1021/jm9903141, 2000.

993 Osada, R., Funkhouser, T., Chazelle, D. and Dobkin, D.: Shape distributions, *ACM Transactions on*
 994 *Graphics*, 21(4), 807 - 832, DOI: 10.1145/571647.571648, 2002

995 Pawson, T.: Dynamic control of signalling by modulator adaptor proteins. *Curr. Opin. Cell Biol.*, 19,
 996 112 - 116, DOI: 10.1016/j.ceb.2007.02.013, 2007.

997 Polakis, P.: Drugging Wnt signaling in cancer. *EMBO J.*, 31, 2737-2746, DOI:
 998 10.1038/emboj.2012.126, 2012.

999 Ponting, C. P., Phillips, C., Davies, K. E. and Blake, D. J.: PDZ domains: targeting signalling
 1000 molecules to submembranous sites. *Bioassays*, 19, 469 - 479, DOI: 10.1002/bies.950190606, 1997.

1001 Puranik, P., Aakanksha, K., Tadas, S. V., Robert, D. B., Lalji, K. G. and Vincent, C. O. N.: Potent
 1002 anti-prostate cancer agents derived from a novel androgen receptor down-regulating agent. *Bioorg.*
 1003 *Med. Chem.*, 16, 3519 - 3529, DOI: 10.1016/j.bmc.2008.02.031, 2008.

1004 [Qin, Y., Feng, L., Fan, X., Zheng, L., Zhang, Y., Chang, L., Li, T.: Neuroprotective Effect of N-
 1005 Cyclohexylethyl-\[A/G\]-\[D/E\]-X-V Peptides on Ischemic Stroke by Blocking nNOS-CAPON
 1006 Interaction. *ACS Chem. Neurosci.* 12\(1\), 244-255, DOI: 10.1021/acchemneuro.0c00739, 2021.](#)

1007 Riese, J., Yu, X., Munnerly, A., Eresh, L., Hsu, S.-C., Grosschedl, R. and Bienz, M.: LEF-1, a nuclear
 1008 factor coordinating signaling inputs from wingless and decapentaplegic. *Cell*, 88, 777 - 787, DOI:
 1009 10.1016/s0092-8674(00)81924-8, 1997.

1010 Rimbault, C., Maruthi, K., Breillat, C., Genuer, C., Crespillo, S., Puente-Muñoz, V., Chamma, I.,
 1011 Gauthereau, I., Antoine, S., Thibaut, C., Tai, F. W. J., Dartigues, B., Grillo-Bosch, D., Claverol, S.,
 1012 Poujol, C., Choquet, D., Mackereth, C. D. and Sainlos, M.: Engineering selective competitors for the
 1013 discrimination of highly conserved protein-protein interaction modules. *Nat. Commun.*, 10, 4521,
 1014 DOI: 10.1038/s41467-019-12528-4, 2019.

hat nach oben verschoben [1]: Lee, I., Choi, S., Yun, J. H.,
 Seo, S. H., Choi, S., Choi, K. Y. and Lee, W.: Crystal structure of the
 PDZ domain of mouse Dishevelled 1 and its interaction with
 CXXC5. *Biochem. Biophys. Res. Commun.*, 485, 584-590, DOI:
 10.1016/j.bbrc.2016.12.023, 2017.

hat gelöscht:

hat formatiert: Englisch (USA)

hat formatiert: Englisch (USA)

1021 Sack, U., Walther, W., Scudiero, D., Selby, M., Aumann, J., Lemos, C., Fichtner, I., Schlag, P. M.,
1022 Shoemaker, R. H. and Stein, U.: S100A4-induced cell motility and metastasis is restricted by the
1023 Wnt/beta-catenin pathway inhibitor calcimycin in colon cancer cells. *Mol. Biol. Cell.*, 22, 3344 -
1024 3354, DOI: 10.1091/mbc.E10-09-0739, 2011.

1025 Sanner, M. F., Olson, A. J. and Spehner, J. C.: Reduced surface: an efficient way to compute molecular
1026 surfaces, *Biopolymers*, 38, 305 – 320, DOI: 10.1002/(SICI)1097-0282(199603)38:3%3C305::AID-
1027 BIP4%3E3.0.CO;2-Y, 1996.

1028 Saube, J., Roske, Y., Schillinger, C., Kamdem, N., Radetzki, S., Diehl, A., Oschkinat, H., Krause, G.,
1029 Heinemann, U. and Rademann, J.: Discovery, structure-activity relationship studies, and crystal
1030 structure of non-peptide inhibitors bound to the Shank3 PDZ domain. *ChemMedChem*, 6, 1411 -
1031 1422, DOI: 10.1002/cmdc.201100094, 2011.

1032 Schultz, J., Hoffmüller, U., Krause, G., Ashurts, J., Macias, M. J., Schmieder, P., Schneider-Mergener,
1033 J. and Oschkinat, H.: Specific interactions between the syntrophin PDZ domain and voltage-gated
1034 sodium channels. *Nat. Struct. Biol.*, 5, 19 – 24, DOI: 10.1038/nsb0198-19, 1998.

1035 [Schwarz-Romond, T., Fiedler, M., Shibata, N., Butler, P.J.G., Kikuchi, A., Higuchi, Y., Bienz, M.:
1036 The DIX domain of Dishevelled confers Wnt signaling by dynamic polymerization. *Nat. Struct. Mol.
1037 Biol.*, 14\(6\), 484-492, DOI: 10.1038/nsmb1247, 2007.](#)

1038 Shan, J., Shi, D. L., Wang, J. and Zheng, J.: Identification of a specific inhibitor of the dishevelled
1039 PDZ domain. *Biochem.*, 44, 15495-15503, DOI: 10.1021/bi0512602, 2005.

1040 Shan, J., Zhang, X., Bao, J., Cassell, R. and Zheng, J. J.: Synthesis of potent Dishevelled PDZ domain
1041 inhibitors guided by virtual screening and NMR studies, *Chem. Biol. Drug. Des.*, 79, 376 – 383,
1042 DOI: 10.1111/j.1747-0285.2011.01295.x, 2012.

1043 Sheng, M. and Sala, C.: PDZ domains and the organization of supramolecular complexes. *Annu. Rev.*
1044 *Neurosci.*, 24, 1 – 29, DOI: 10.1146/annurev.neuro.24.1.1, 2001.

1045 Sievers, F., Wilm, A., Dineen, D. G., Gibson, T. J., Karplus, K., Li, W., Lopez, R., McWilliam, H.,
1046 Rimmert, M., Söding, J., Thompson, J. D. and Higgins, D. G.: Fast, Scalable generation of high-
1047 quality protein multiple sequence alignments using Clustal Omega. *Mol. Syst. Biol.*, 7, 539,
1048 Doi:10.1038/msb.2011.75, 2011.

1049 Sineva, G. S. and Pospelov, V. A.: Inhibition of GSK3beta enhances both adhesive and signalling
1050 activities of beta-catenin in mouse embryonic stem cells. *Biol. Cell*, 102, 549-560, DOI:
1051 10.1042/BC20100016, 2010.

1052 Sleight, A. J., Boess, F. G., Bös, M., Levet-Trafit, B., Riemer, C. and Bourson, A. Br.:
1053 Characterization of Ro 04-6790 and Ro 63-0563: potent and selective antagonists at human and rat
1054 5-HT6 receptors. *J. Pharmacol.*, 124, 556 - 562, DOI: 10.1038/sj.bjp.0701851, 1998.

1055 Songyang, Z., Fanning, A. S., Fu, C., Xu, J., Marfatia, S. M., Chisti, A. H., Crompton, A., Chan, A.
1056 C., Anderson, J. M. and Cantley, L. C.: Recognition of unique carboxyl-terminals motifs by distinct
1057 PDZ domains. *Science*, 275, 73 - 77, DOI: 10.1126/science.275.5296.73, 1997.

1058 Shuker, S. B., Hajduk, P. J., Meadows, R. P. and Fesik, S. W.: Discovering high-affinity ligands for
1059 proteins: SAR by NMR. *Science*, 274, 1531 – 1534, DOI: 10.1126/science.274.5292.1531, 1996.

1060 Shuker, S. B., Hajduk, P. J., Meadows, R. P. and Fesik, S. W.: Discovering high-affinity ligands for
1061 proteins: SAR by NMR. *Science*, 274, 1531 – 1534, DOI: 10.1126/science.274.5292.1531, 1996.

1062 Tellew, J. E., Baska, R. A. F., Beyer, S. M., Carlson, K. E., Cornelius, L. A., Fadnis, L., Gu, Z., Kunst,
1063 B. L., Kowala, M. C., Monshizadegan, H., Murugesan, N., Ryan, C. S., Valentine, M. T., Yang, Y.
1064 and Macor, J. E.: Discovery of 4-[(imidazol-1-yl)methyl]biphenyl-2-sulfonamides as dual
1065 endothelin/angiotensin II receptor antagonists. *Bioorg. Med. Chem. Letters*, 13, 1093 – 1096, DOI:
1066 10.1016/S0960-894X(03)00018-0, 2003.

1067 [The PyMOL Molecular Graphics System, Version 2.3.4 Schrödinger, LLC](#)

1068 Uematsu, K., He, B., You, L., Xu, Z., McCormick, F. and Jablons, D. M.: Activation of the Wnt
1069 pathway in non-small cell lung cancer: evidence of dishevelled overexpression. *Oncogene*, 22, 7218
1070 - 7221, DOI: 10.1038/sj.onc.1206817, 2003.

1071 Uematsu, K., Kanazawa, S., You, L., He, B., Xu, Z., Li, K., Peterlin, B. M., McCormick, F. and
1072 Jablons, D. M.: Wnt pathway activation in mesothelioma: evidence of dishevelled overexpression and
1073 transcriptional activity of β -catenin. *Cancer Res.*, 63, 4547 – 4551, 2003.

1074 Vermeulen, L., De Sousa E Melo, F., van der Heijden, M., Cameron, K., de Jong, J. H., Borovski, T.,
1075 Tuynman, J. B., Todaro, M., Merz, C., Rodermond, H., Sprick, M. R., Kemper, K., Richel, J. J.,

hat formatiert: Englisch (USA)

Feldfunktion geändert

1076 Stassi, G. and Medema, J. P.: Wnt activity defines colon cancer stem cells and is regulated by the
1077 microenvironment. *Nat. Cell. Biol.*, 12, 468 - 476, DOI: 10.1038/ncb2048, 2010.
1078 Wallingford, B. J. and Raymond H.: The developmental biology of Dishevelled: an enigmatic protein
1079 governing cell fate and cell polarity. *Development*, 132, 4421 - 4436, DOI: 10.1242/dev.02068,
1080 2005.
1081 Wang, C., Dai, J., Sun, Z., Shi, C., Cao, H., Chen, X., Gu, S., Li, Z., Qian, W. and Han, X.: Targeted
1082 inhibition of dishevelled PDZ domain via NSC668036 depresses fibrotic process. *Exp. Cell Res.*,
1083 331, 115 - 122, DOI: 10.1016/j.yexcr.2014.10.023, 2015.
1084 Weeraratna, A. T., Jiang, Y., Hostetter, G., Rosenblatt, K., Duray, P., Bittner, M. and Trent, J. M.:
1085 Wnt5a signalling directly affects cell motility and invasion of metastatic melanoma. *Cancer Cell*, 1,
1086 279 - 288, DOI: 10.1016/s1535-6108(02)00045-4, 2002.
1087 Wong, H. C., Bourdelas, A., Krauss, A., Lee, H. J., Shao, Y., Wu, D., Mlodzik, M., Shi, D. L. and
1088 Zheng, J.: Direct binding of the PDZ domain of Dishevelled to a conserved internal sequence in the
1089 C-terminal region of Frizzled J. *Mol. Cell*, 12, 1251 -1260, DOI: 10.1016/s1097-2765(03)00427-1,
1090 2003.
1091 Wong, H., Mao, J., Nguyen, J. T., Srinivas, S., Zhang, W., Liu, B., Li, L., Wu, D. and Zheng, J.:
1092 Structural basis of the recognition of the dishevelled DEP domain in the Wnt signalling pathway.
1093 *Nat. Struct. Biol.*, 7, 1178 -1184, DOI: 10.1038/82047, 2000.
1094 Wu, C., Decker, E. R., Blok, N., Bui, H., Chen, Q., Raju, B., Bourgoyne, A. R., Knowles, V.,
1095 Biediger, R. J., Market, R. V., Lin, S., Dupre, B., Kogan, T. P., Holland, G. W., Brock, T. A. and
1096 Dixon, R. A. F.: Endothelin antagonists: substituted mesitylcarboxamides with high potency and
1097 selectivity for ET(A) receptors. *J. Med. Chem.*, 42, 4485 - 4499, DOI: 10.1021/jm9900063, 1999.
1098 Zartler, E. R. and Shapiro, M. J.: Protein NMR-based screening in drug discovery. *Curr. Pharm. Des.*,
1099 12, 3963 - 3972, DOI: 10.2174/138161206778743619, 2006.
1100 Zartler, E. R., Hanson, J., Jones, B. E., Kline, A. D., Martin, G., Mo, H., Shapiro, M. J., Wang, R.,
1101 Wu, H. and Yan, J.: RAMPED-UP NMR: multiplexed NMR-based screening for drug discovery. *J.*
1102 *Am. Chem. Soc.*, 125, 10941 - 10946, DOI: 10.1021/ja0348593, 2003.
1103 Zhang, M. and Wang, W.: Organization of signalling complexes by PDZ-domain scaffold proteins.
1104 *Acc. Chem. Res.*, 36, 530 - 538, DOI: 10.1021/ar020210b, 2003.
1105 Zhang, M. and Wang, W.: Organization of signalling complexes by PDZ-domain scaffold proteins.
1106 *Acc. Chem. Res.*, 36, 530 - 538, DOI: 10.1021/ar020210b, 2003.
1107 Zhang, Y., Appleton, B. A., Wiesmann, C., Lau, T., Costa, M., Hannoush, R. N. and Sidhu, S. S.:
1108 Inhibition of Wnt signaling by Dishevelled PDZ peptides. *Nat. Chem. Biol.*, 5, 217 -219, DOI:
1109 10.1038/nchembio.152, 2009.